

AD-A085 185

PENNSYLVANIA STATE UNIV UNIVERSITY PARK APPLIED RESE--ETC F/6 20/1
NONLINEAR ACOUSTIC WAVE INTERACTIONS IN LAYERED MEDIA. (U)

MAR 80 D M YEAGER

N00024-79-C-6043

NL

UNCLASSIFIED

1 of 2

3/8/80

3/8/80

3/8/80

3/8/80

3/8/80

3/8/80

3/8/80

3/8/80

3/8/80

3/8/80

3/8/80

3/8/80

3/8/80

3/8/80

3/8/80

3/8/80

3/8/80

3/8/80

3/8/80

3/8/80

3/8/80

3/8/80

3/8/80

3/8/80

3/8/80

3/8/80

3/8/80

3/8/80

3/8/80

3/8/80

3/8/80

3/8/80

3/8/80

3/8/80

3/8/80

3/8/80

3/8/80

3/8/80

3/8/80

3/8/80

3/8/80

3/8/80

3/8/80

3/8/80

3/8/80

3/8/80

3/8/80

3/8/80

3/8/80

3/8/80

3/8/80

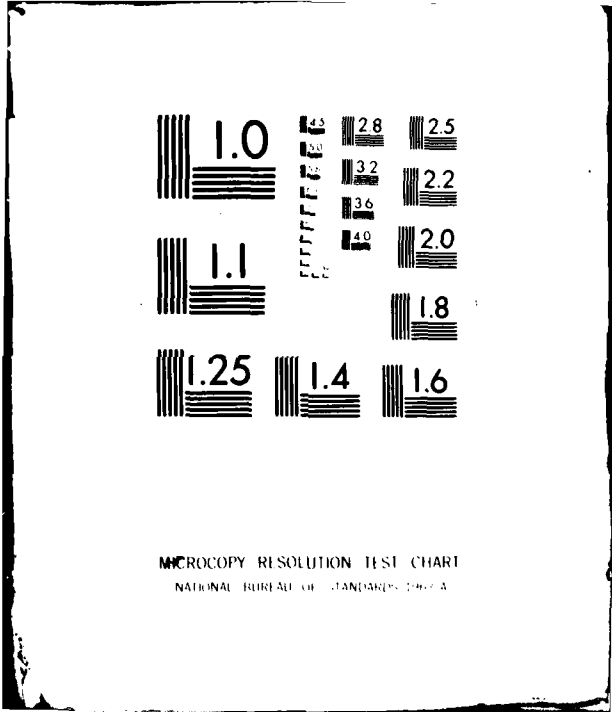
3/8/80

3/8/80

3/8/80

3/8/80

3/8/80



ADA 085185

(2) ~~SECRET~~

NONLINEAR ACOUSTIC WAVE INTERACTIONS
IN LAYERED MEDIA

David Marvin Yeager

Technical Memorandum
File No. TM 80-32
March 6, 1980
Contract No. N00024-79-C-6043

Copy No. 6

DTIC
SELECTED
JUN 9 1980

A

The Pennsylvania State University
Institute for Science and Engineering
APPLIED RESEARCH LABORATORY
Post Office Box 30
State College, PA 16801

APPROVED FOR PUBLIC RELEASE
DISTRIBUTION UNLIMITED

NAVY DEPARTMENT
NAVAL SYSTEMS COMMAND

80 6 6 124

DDC FILE COPY

UNCLASSIFIED

SECURITY CLASSIFICATION OF THIS PAGE (When Data Entered)

REPORT DOCUMENTATION PAGE		READ INSTRUCTIONS BEFORE COMPLETING FORM
1. REPORT NUMBER (14) TM-80-32	2. GOVT ACCESSION NO. AN-A085 185	3. RECIPIENT'S CATALOG NUMBER
4. TITLE (and Subtitle) (6) NONLINEAR ACOUSTIC WAVE INTERACTIONS IN LAYERED MEDIA		5. TYPE OF REPORT & PERIOD COVERED MS Thesis, May 1980
7. AUTHOR(s) (10) David Marvin/Yeager		6. PERFORMING ORG. REPORT NUMBER TM 80-32
9. PERFORMING ORGANIZATION NAME AND ADDRESS The Pennsylvania State University Applied Research Laboratory Post Office Box 30, State College, PA 16801		8. CONTRACT OR GRANT NUMBER(s) (15) N00024-79-C-6043
11. CONTROLLING OFFICE NAME AND ADDRESS Naval Sea Systems Command Department of the Navy Washington, DC 20362		10. PROGRAM ELEMENT, PROJECT, TASK AREA & WORK UNIT NUMBERS (11) 6 MAR 80
14. MONITORING AGENCY NAME & ADDRESS (if different from Controlling Office) (12) 109		12. REPORT DATE March 6, 1980
		13. NUMBER OF PAGES 107 pages & figures
		15. SECURITY CLASS. (of this report) Unclassified, Unlimited
		15a. DECLASSIFICATION/DOWNGRADING SCHEDULE
16. DISTRIBUTION STATEMENT (of this Report) Approved for public release, distribution unlimited per NSSC (Naval Sea Systems Command), 4/9/80		
17. DISTRIBUTION STATEMENT (of the abstract entered in Block 20, if different from Report) (9) Technical memo.		
18. SUPPLEMENTARY NOTES		
19. KEY WORDS (Continue on reverse side if necessary and identify by block number) acoustic, waveguide, dispersion, conversion, efficiency, thesis		
20. ABSTRACT (Continue on reverse side if necessary and identify by block number) The conversion efficiency of parametric amplification in fluids is low because of the low dispersivity. A discontinuous change in phase velocity at the boundary of a waveguide introduces dispersion, which in turn affects conversion efficiency. It is the purpose of this thesis to develop from first principles an analytical model which may be used to numerically predict the conversion efficiency of a flat-plate, acoustic waveguide given		

DD FORM 1473
1 JAN 73

EDITION OF 1 NOV 68 IS OBSOLETE
S/N 0102-LF-014-6601

391 007

UNCLASSIFIED

SECURITY CLASSIFICATION OF THIS PAGE (When Data Entered)

UNCLASSIFIED

SECURITY CLASSIFICATION OF THIS PAGE (When Data Entered)

20. ABSTRACT (continued)

the physical parameters of the system.

In order to quantify weak, finite-amplitude interactions in the guide, the linear behavior of the system must first be analyzed. This is accomplished using Green's functions. Once the linear characteristics have been determined, nonlinear phenomena are investigated; both analytically and numerically via digital computer graphics. The physical parameters in the numerical examples were chosen to correspond with materials used in previously published experimental work using cylinders rather than flat plates.

Accession For	
1. Title	<input checked="" type="checkbox"/>
2. Author	<input type="checkbox"/>
3. Subject	<input type="checkbox"/>
4. Summary	<input type="checkbox"/>
5. Other	<input type="checkbox"/>
6. Distribution	<input type="checkbox"/>
7. Other	<input type="checkbox"/>
8. Other	<input type="checkbox"/>
9. Other	<input type="checkbox"/>
10. Other	<input type="checkbox"/>
11. Other	<input type="checkbox"/>
12. Other	<input type="checkbox"/>
13. Other	<input type="checkbox"/>
14. Other	<input type="checkbox"/>
15. Other	<input type="checkbox"/>
16. Other	<input type="checkbox"/>
17. Other	<input type="checkbox"/>
18. Other	<input type="checkbox"/>
19. Other	<input type="checkbox"/>
20. Other	<input type="checkbox"/>
21. Other	<input type="checkbox"/>
22. Other	<input type="checkbox"/>
23. Other	<input type="checkbox"/>
24. Other	<input type="checkbox"/>
25. Other	<input type="checkbox"/>
26. Other	<input type="checkbox"/>
27. Other	<input type="checkbox"/>
28. Other	<input type="checkbox"/>
29. Other	<input type="checkbox"/>
30. Other	<input type="checkbox"/>
31. Other	<input type="checkbox"/>
32. Other	<input type="checkbox"/>
33. Other	<input type="checkbox"/>
34. Other	<input type="checkbox"/>
35. Other	<input type="checkbox"/>
36. Other	<input type="checkbox"/>
37. Other	<input type="checkbox"/>
38. Other	<input type="checkbox"/>
39. Other	<input type="checkbox"/>
40. Other	<input type="checkbox"/>
41. Other	<input type="checkbox"/>
42. Other	<input type="checkbox"/>
43. Other	<input type="checkbox"/>
44. Other	<input type="checkbox"/>
45. Other	<input type="checkbox"/>
46. Other	<input type="checkbox"/>
47. Other	<input type="checkbox"/>
48. Other	<input type="checkbox"/>
49. Other	<input type="checkbox"/>
50. Other	<input type="checkbox"/>
51. Other	<input type="checkbox"/>
52. Other	<input type="checkbox"/>
53. Other	<input type="checkbox"/>
54. Other	<input type="checkbox"/>
55. Other	<input type="checkbox"/>
56. Other	<input type="checkbox"/>
57. Other	<input type="checkbox"/>
58. Other	<input type="checkbox"/>
59. Other	<input type="checkbox"/>
60. Other	<input type="checkbox"/>
61. Other	<input type="checkbox"/>
62. Other	<input type="checkbox"/>
63. Other	<input type="checkbox"/>
64. Other	<input type="checkbox"/>
65. Other	<input type="checkbox"/>
66. Other	<input type="checkbox"/>
67. Other	<input type="checkbox"/>
68. Other	<input type="checkbox"/>
69. Other	<input type="checkbox"/>
70. Other	<input type="checkbox"/>
71. Other	<input type="checkbox"/>
72. Other	<input type="checkbox"/>
73. Other	<input type="checkbox"/>
74. Other	<input type="checkbox"/>
75. Other	<input type="checkbox"/>
76. Other	<input type="checkbox"/>
77. Other	<input type="checkbox"/>
78. Other	<input type="checkbox"/>
79. Other	<input type="checkbox"/>
80. Other	<input type="checkbox"/>
81. Other	<input type="checkbox"/>
82. Other	<input type="checkbox"/>
83. Other	<input type="checkbox"/>
84. Other	<input type="checkbox"/>
85. Other	<input type="checkbox"/>
86. Other	<input type="checkbox"/>
87. Other	<input type="checkbox"/>
88. Other	<input type="checkbox"/>
89. Other	<input type="checkbox"/>
90. Other	<input type="checkbox"/>
91. Other	<input type="checkbox"/>
92. Other	<input type="checkbox"/>
93. Other	<input type="checkbox"/>
94. Other	<input type="checkbox"/>
95. Other	<input type="checkbox"/>
96. Other	<input type="checkbox"/>
97. Other	<input type="checkbox"/>
98. Other	<input type="checkbox"/>
99. Other	<input type="checkbox"/>
100. Other	<input type="checkbox"/>

Disc

UNCLASSIFIED

SECURITY CLASSIFICATION OF THIS PAGE (When Data Entered)

ABSTRACT

The conversion efficiency of parametric amplification in fluids is low because of the low dispersivity. A discontinuous change in phase velocity at the boundary of a waveguide introduces dispersion, which in turn affects conversion efficiency. It is the purpose of this thesis to develop from first principles an analytical model which may be used to numerically predict the conversion efficiency of a flat-plate, acoustic waveguide given the physical parameters of the system.

To quantify weak, finite-amplitude interactions in the guide, the linear behavior of the system is analyzed using Green's functions. Once the linear characteristics have been determined, nonlinear phenomena are investigated, both analytically and numerically via digital computer graphics. The physical parameters in the numerical examples are chosen to correspond with materials used in previously published experimental work using cylinders rather than flat plates.

CONTENTS

	Page
ABSTRACT.	iii
LIST OF FIGURES	vi
LIST OF SYMBOLS	viii
ACKNOWLEDGEMENTS.	x
Chapter	
I. INTRODUCTION.	1
1.1 Parametric Arrays.	1
1.2 Statement of Problem	7
1.3 Theoretical Framework.	10
1.4 Literature Review.	12
1.5 Outline of the Analytical Approach	14
II. GREEN'S FUNCTIONS	16
2.1 Definition	16
2.2 Velocity Potential in Terms of Green's Functions.	17
2.3 Derivation of G_{χ}	19
2.4 Inverse Transformation of G_{χ}	27
2.5 Discussion of Poles of G_{χ}	29
2.6 Contour Integration.	32
2.7 Evaluation of Residues	35
2.8 Boundary-Induced Dispersion.	38

III.	NONLINEAR WAVE INTERACTIONS IN LAYERED MEDIA. . .	41
3.1	Introduction	41
3.2	Frequency-Domain Solution.	44
3.3	Source Distribution.	46
3.4	Evaluation of $\phi_{\omega_{\pm}}$	48
IV.	NUMERICAL ANALYSIS.	52
4.1	Determination of Axial Wavenumber.	52
4.2	Mode Shapes.	54
4.3	Behavior of Nonlinearly Generated Components in Dispersive Media.	62
4.4	Dispersion in Medium II.	68
V.	CONCLUSIONS	72
APPENDICES		
A.	DETERMINATION OF $\frac{\partial \Psi}{\partial \chi} \Big _{\chi=\chi_m}$	74
B.	PLANE-WAVE MODE	76
C.	GREEN'S FUNCTIONS FOR MEDIA I AND III	79
D.	NUMERICAL EVALUATION OF EIGENVALUES: COMPUTER PROGRAM LISTING.	88
	BIBLIOGRAPHY.	95

LIST OF FIGURES

Figure	Page
1. Spectral Amplitude Variation with Range of a Monotonic, Finite-Amplitude Wave and Self-Generated Harmonics in an Inviscid, Dispersionless Fluid	4
2. Spectral Amplitude Variation with Range of a Bifrequency, Finite-Amplitude Wave and Self-Generated Components in a Viscous, Dispersionless Fluid	5
3. Propagation of Plane Wave Trapped in Medium II.	8
4. Modes of Propagation in an Acoustic Waveguide for Real Axial Wavenumber.	30
5. Contour Integration in Complex Axial Wavenumber (χ) Plane Around the Poles $\pm\chi_m$ for $z \geq z'$ and $z \leq z'$	34
6. Dispersion Relationship for First Few Guided Modes in a 0.1-m.-Thick Slab of Silicone Rubber Immersed in Water	40
7. Dispersion Relationship for First Few Guided Modes in a 0.1-m.-Thick Waveguide Bounded by Semi-Hard Media.	55
8. Dispersion Relationship for First Few Guided Modes in a 0.1-m.-Thick Waveguide Bounded by Semi-Soft Media.	56
9. Transverse Pressure Distribution in Medium II at Fixed Range for $m=1$ Mode at 5, 10, and 15 kHz	59

10.	Transverse Pressure Distribution in Medium II at Fixed Range for $m=2$ Mode at 10, 15, and 20 kHz	60
11.	Transverse Pressure Distribution in Medium II at Fixed Range for $m=3$ Mode at 15, 20, and 25 kHz	61
12.	Transverse Pressure Distribution in Medium II for $m=1$ Mode for a 0.1-m.-Thick Slab of Varying Density Immersed in Water at 8kHz.	63
13.	Magnitude of Axial Component of Velocity Potential, Z , in Medium II as Given by Equation (3-17) for Several Values of Real Δ_z ($=1,2,4,8$), Hence, Damping Is Neglected (i.e., $\alpha=0$)	65
14.	Magnitude of Axial Component of Velocity Potential, Z , in Medium II as Given by Equation (4-14) for $\Delta_z=4.0$ with Increasing Amounts of Absorption.	69
15.	Variation of Δ_z with Difference Frequency (f_-) for Fixed Ratio of Primary Frequency (f_1) to f_- (i.e., $f_1/f_-=10.0$)	71
16.	FORTTRAN Listing of Root-Finding Computer Program AXIAL.	90

LIST OF SYMBOLS

a	waveguide thickness (medium II)
c	adiabatic small-signal-speed-of-sound
$\tilde{\mathbf{k}} = \omega/c$	free-space wavenumber vector
$\tilde{\mathbf{v}}$	particle velocity vector
v_n	particle velocity component normal to waveguide boundary
\tilde{v}_ω	frequency-domain particle velocity
t	time
G_ω	Green's function (frequency space)
G_m^+	frequency-domain Green's function for m^{th} forward-guided mode
G_χ	Green's function (wavenumber space)
S_ω	source distribution for frequency ω
p	pressure
(x', z')	point source coordinate
$A_1, B_1, B_2, C_1, C_2, D_2$	coefficients for Green's function in various transverse regions
i	$\sqrt{-1}$
$\text{Im}(X)$	imaginary part of a complex value X
$\text{Re}(X)$	real part of a complex value X
$\text{RES}(F)$	residue of function F
q, s, m	subscripts used to designate primary and difference frequency modes
X	transverse component of velocity potential (3-12)
Z	axial component of velocity potential (3-13)
f	frequency

$\tilde{\nabla}$	del vector operator
∇^2	Laplacian operator
ϕ	velocity potential, time domain
ϕ_ω	velocity potential, frequency domain
ω	angular frequency
ω_1, ω_2	angular frequency of primary waves
ω_\pm	angular sum or difference frequency
κ	transverse wavenumber component
χ	axial wavenumber component
χ_m	axial wavenumber for m^{th} guided mode
δ	Dirac delta function
ρ	density
ϵ	acoustic mach number
$\Psi(X)$	determinant of matrix (2-14)
$\Psi'(X_m)$	derivative of Ψ with respect to χ evaluated at X_m
π	constant 3.1415...
γ	specific heat ratio in gases ($1 + \frac{B}{A}$ in liquids)
Δ_x, Δ_z	transverse and axial wavenumber difference
$\tilde{\Delta}$	free-space wavenumber difference vector
α	attenuation coefficient
Γ	acoustic Reynolds number
β	coefficient of nonlinearity

ACKNOWLEDGEMENTS

The author wishes to express his sincere gratitude to Dr. Francis H. Fenlon without whose inspiration and dedication this thesis would not have been possible. In addition, Francis S. McKendree is gratefully acknowledged for his assistance with the computer programs utilized in the section on numerical analysis.

This research was supported by the Applied Research Laboratory of The Pennsylvania State University under contract with the U.S. Naval Sea Systems Command.

Chapter I

INTRODUCTION

The interaction of finite-amplitude acoustic waves in layered media differs significantly from free-field behavior. In order to investigate these differences, the properties of nonlinear acoustic wave interactions in unbounded media must first be considered. In order to address this issue, therefore, the thesis begins by comparing the relative advantages and disadvantages of parametric and conventional linear transducers.

1.1 Parametric Arrays

According to linear acoustic theory, the propagation of a disturbance in an isotropic, homogeneous medium is governed by the linear wave equation:

$$(1-1) \quad (\nabla^2 - c_0^{-2} \frac{\partial^2}{\partial t^2}) \phi = 0$$

where the Laplacian ∇^2 and the term $c_0^{-2} \frac{\partial^2}{\partial t^2}$ operate linearly on the the velocity potential ϕ . Hence, the spectrum of any wave must remain constant as the disturbance propagates through the acoustic medium. In order to obtain Equation (1-1), all second- and higher-order terms of the velocity potential have been neglected. Whether this is a "safe" assumption or not depends on the value of the acoustic mach number ϵ and the absorption characteristics of the medium.¹ In an inviscid fluid, nonlinearity plays a role at any value of ϵ . Moreover, in a viscous fluid, $\epsilon=0.1$ is the limit above which second-order theory begins to fail.²

The governing finite-amplitude wave equation with second-order terms included is given in Chapter III. It is sufficient to note here, that the distortion of a propagating waveform and a consequent change in its spectrum as a function of range are described by these terms. For example, an initially monotonic, finite-amplitude disturbance of frequency ω_1 in a lossless medium will eventually become a sawtooth wave, the spectrum of which contains all harmonics of the sinusoid. The growth of these

¹ $\epsilon = \frac{u}{c}$, where u is the particle velocity, and c is the small signal speed of sound.

² A more viable measure of the manifestation of nonlinear behaviour in a lossy medium is provided by the acoustic Reynolds number which, for plane waves, assumes the form $\Gamma = \beta \epsilon k / \alpha$ which gives a ratio of nonlinearity to absorption (viscosity) loss per wavelength. If $\Gamma \geq 1$, then nonlinear effects become dominant. See also Rudeenko and Soluyan, p. 11.

nonlinearly generated components is at the expense of the amplitude of the fundamental (energy is, of course, conserved in a inviscid fluid) as shown in Figure 1 for the case of an initially monotonic wave in an inviscid dispersionless fluid.

For the case of an initially bifrequency waveform (frequencies ω_1 and ω_2), not only are harmonics of each fundamental generated, but interaction between the two fundamentals produces intermodulation components as well. Figure 2 schematically depicts the growth and decay of several components with range. Increased absorption at higher frequencies is reflected in the sketch where the lowest possible spectral component, the difference frequency ω_- , continues to propagate after the higher frequencies have been absorbed. Thus, the medium has the effect of a low-pass filter.³

The term "parametric array" refers to the finite-amplitude generation of these intermodulation frequency components by a bifrequency source. The "length" of the array refers to the region of interaction within which energy is transferred from the primary waves to the nonlinearly generated components.

Parametric arrays are highly directional. For example, the half-power beamwidth of a nonlinearly generated

³This is only true of thermo-viscous fluids.

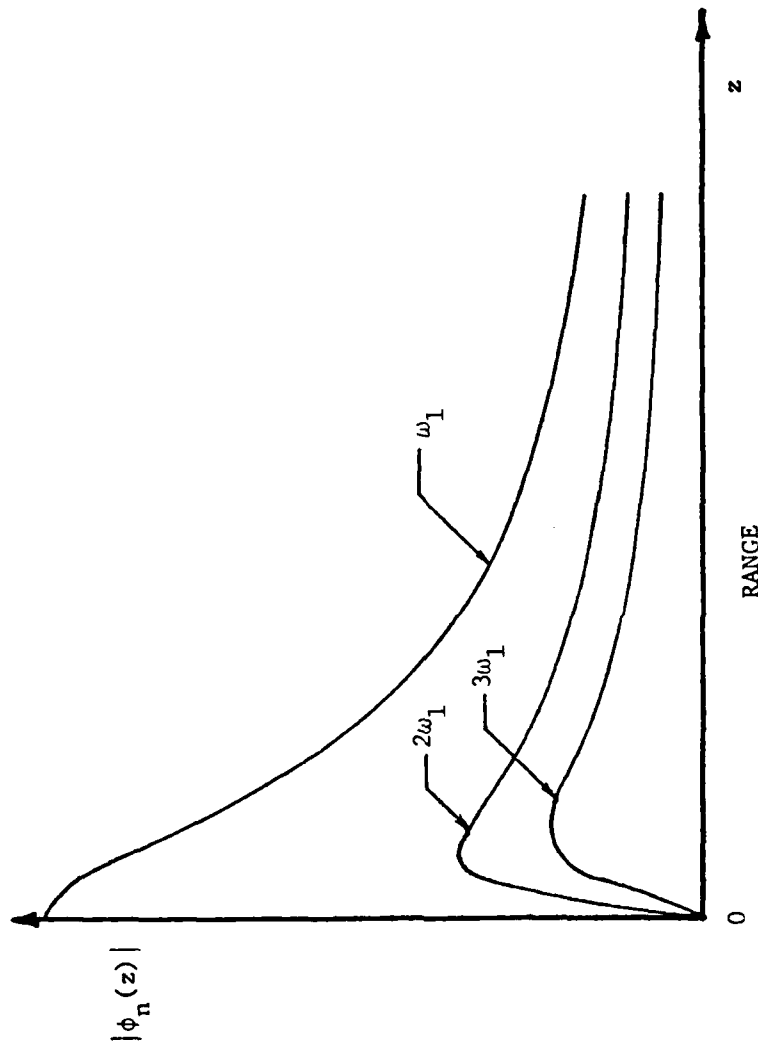


Figure 1. Spectral amplitude variation with range of a monotonic, finite-amplitude wave and self-generated harmonics in an inviscid, dispersionless fluid.⁴

⁴D.T. Blackstock, "Connection Between the Fay and Fubini Solutions for Plane Sound Waves of Finite-Amplitude," Journal of the Acoustical Society of America, 39 (1966), 1019-1026.

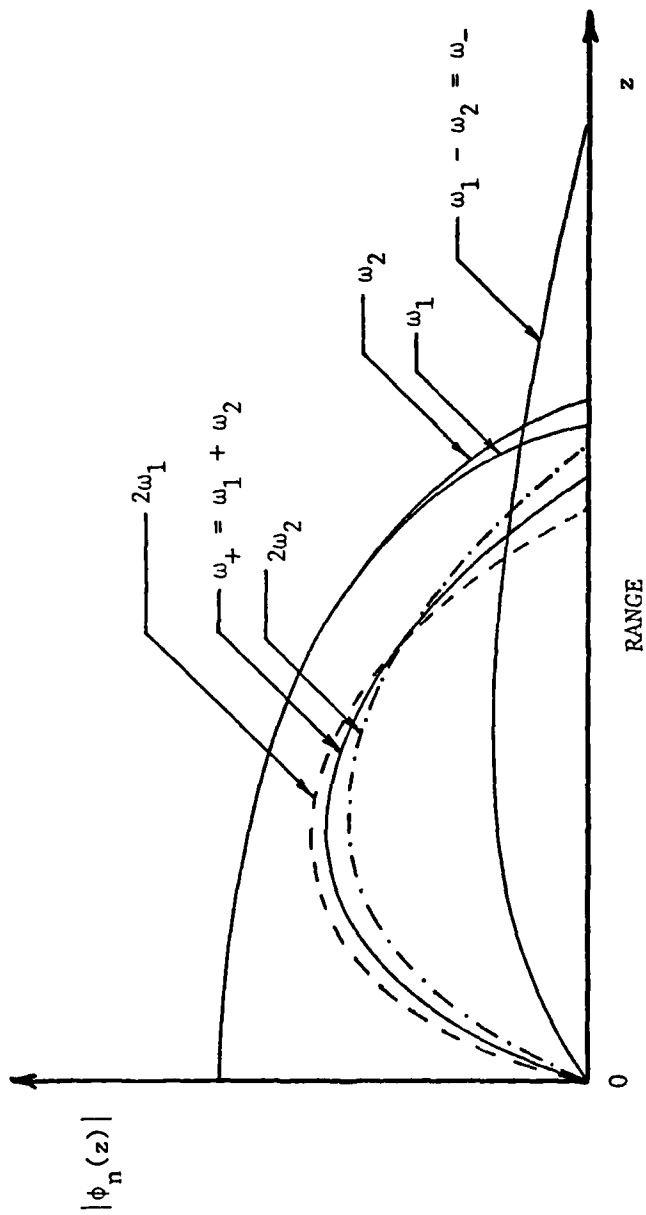


Figure 2. Spectral amplitude variation with range of a bifrequency, finite-amplitude wave and self-generated components in a viscous, dispersionless fluid.⁵

⁵F.H.Fenlon, private communication, August 6, 1976.

difference frequency is considerably narrower than if generated directly by a conventional piston projector radiating at the same frequency; i.e., in order to produce the same beamwidth conventionally, a much larger transducer aperture would be required.

However, a major factor inhibiting more extensive use of parametric arrays is their low conversion efficiency. "Conversion efficiency" refers to the ratio of energy transferred to the difference-frequency component versus the amount of energy initially entering the system via the primary waves. In a nondispersive fluid, transferred energy is divided among all nonlinearly generated components, only a small fraction being supplied to the difference frequency. However in a dispersive medium where phase velocity is a function of frequency, some components will interact resonantly, thus increasing in amplitude with range, while others will be excited asynchronously producing the spatial beating effect described in Chapter IV. Under such circumstances, a limited amount of energy will be transmitted to those components which are nonresonantly excited, since their amplitudes never exceed a maximum value where synchronous interactions are limited only by the initial strength of the primary fields.

1.2 Statement of Problem

As stated above, a dispersive medium is one in which the phase velocity of a monotonic disturbance is a function of frequency. Dispersion may be "medium-induced" (e.g., via internal relaxation mechanisms or inhomogeneities such as air bubbles in water or embedded in rubber) or "boundary-induced", the latter resulting from discontinuities in density and bulk speed of sound at the interfaces between two media.

Figure 3 depicts a three-layered acoustic medium where the discontinuities at $x=a$ and $x=0$ represent the boundaries of a flat-plate waveguide (medium II). Some of the energy entering medium II will be internally reflected at the upper and lower interfaces as it propagates in the positive z -direction. It will be shown that the speed at which this trapped energy propagates through the guide depends not only upon which mode it is in, but also upon the frequency of the disturbance. Therefore, if parametric interaction occurs in a waveguide, where dispersion is induced by the boundaries, certain spectral components will interact resonantly while others will be asynchronously excited.

It is the purpose of this investigation to develop expressions which may be used to analytically determine the extent to which the boundary-induced dispersion of a waveguide can enhance the conversion efficiency of certain

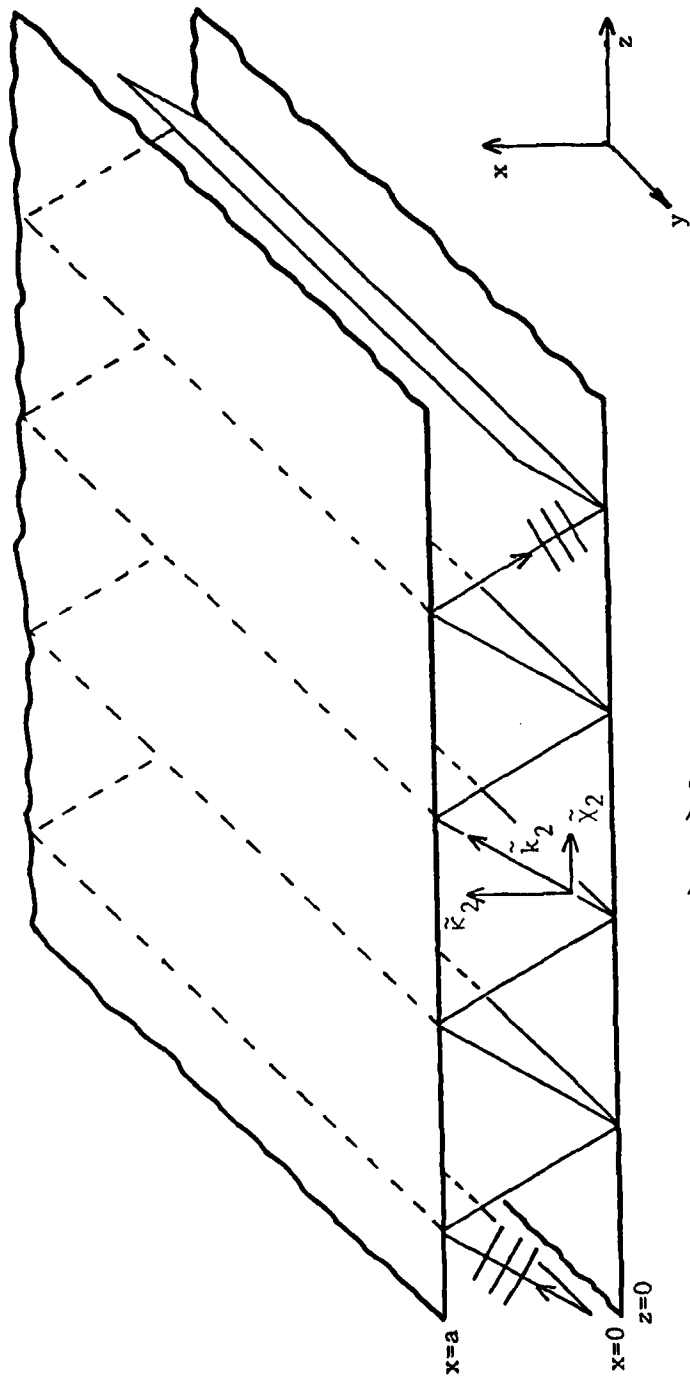
$\rho_1 c_1$ $\rho_2 c_2$ $\rho_3 c_3$ 

Figure 3. Propagation of plane wave trapped in medium II. Semi-infinite planes at $x=0$ and $x=a$ represent fluid-fluid interface and between II and I, respectively.

nonlinearly generated frequency components, namely, the sum and difference frequencies. The investigation is conducted in two distinct parts. First, exact analytic expressions are derived to clearly define the dispersive relationships of an acoustic, slow waveguide sandwiched between two semi-infinite media of arbitrary characteristic impedances. Second, once these relationships are established, the effects of dispersion on specific nonlinearly generated intermodulation components can then be evaluated for various physical systems. To make this evaluation, expressions for the sum and difference frequency velocity potentials of an initially bifrequency wave are found via the derivation of Green's functions.

It should be noted that the equations representing the velocity potential for the sum and difference frequencies inside the guide (see Chapter III) contain terms which grow linearly without bounds as the wave propagates through the waveguide. These components, which are referred to as "secular terms", occur for the case of resonant interaction in a lossless medium. This physical inconsistency is heuristically explained in Chapter IV. However, to define the bounds of resonantly excited components, constrained perturbation theory may be applied to the problem (e.g., the method of strained parameters),⁶ a task that remains a future research objective.

⁶A.H. Nayfeh, Perturbation Methods (New York: Wiley-Interscience, 1973), Section 3.1.

1.3 Theoretical Framework

The sketch shown in Figure 3 represents a flat-plate, acoustic, slow waveguide (medium II) of finite thickness "a" sandwiched between two semi-infinite, homogeneous, fluid half-spaces of arbitrary characteristic impedances $\rho_1 c_1$ and $\rho_3 c_3$, where ρ denotes density and c denotes phase velocity. The fluid-fluid interfaces at $x=0$ and $x=a$ extend infinitely in the positive and negative y -directions and semi-indefinitely in the positive z -direction. The term "fluid" is used in this context to describe a medium having a shear modulus low enough to neglect the effect of shear waves, thus permitting only compressional wave propagation to be considered. Gases, most liquids, and some silastic rubbers exhibit this property. It is also assumed that the free-field phase velocity in medium II, i.e., the sandwiched layer, is less than that in either medium I or III. Without loss of generality, it is assumed that

$$(1-2) \quad c_3 > c_1 > c_2 \quad ,$$

where c_i ($i=1,2,3$) represents phase velocity in medium "i".

As shown in Figure 3, the wavenumber vector \tilde{k}_i normal to the plane wavefront is decomposed into transverse and axial components (κ_i and χ_i , respectively) such that

$$(1-3) \quad |\tilde{k}_i|^2 = \left(\frac{\omega}{c_i}\right)^2 = \kappa_i^2 + \chi_i^2 \quad ,$$

where ω represents angular frequency ($\omega=2\pi f$). The horizontal y-component is assumed to be zero; hence, the investigation is a two-dimensional problem. The governing Helmholtz equation for a harmonic field $\exp(-i\omega t)$ in medium II is

$$(1-4) \quad (\nabla^2 + k_2^2) \phi_\omega = 0 ,$$

where the Laplacian ∇^2 in rectangular coordinates is given by:

$$(1-5) \quad \nabla^2 = \frac{\partial^2}{\partial x^2} + \frac{\partial^2}{\partial z^2} ; \left(\frac{\partial}{\partial y} = 0 \right) ,$$

and the velocity potential in the frequency domain ϕ_ω is

$$(1-6) \quad \tilde{v} = \tilde{\nabla} \phi_\omega(x, z) \exp(-i\omega t)$$

or

$$(1-7) \quad \tilde{v}_\omega = \tilde{\nabla} \phi_\omega(x, z) ,$$

where

$$(1-8) \quad \tilde{\nabla} = \frac{\partial}{\partial x} \tilde{i} + \frac{\partial}{\partial z} \tilde{k} ; \left(\frac{\partial}{\partial y} = 0 \right) .$$

Notice that the unit vector in the z-direction \tilde{k} in Equation (1-8) is not related to the free-space wavenumber vector \tilde{k} in Equations (1-3) and (1-4).

1.4 Literature Review

Nonlinear wave interactions in a dispersive medium have been investigated by Nayfeh and Tsai⁷ in order to evaluate the nonlinear effects of the gas and lining material in a duct. They determined a third-order uniform expansion using the method of multiple scales⁸ to analyze the nonlinear effects on the propagation and attenuation of all existing modes in a two-dimensional, hard-walled duct lined with an acoustical material. Vaidya and Wang⁹ utilized a second-order expansion to determine the spectral energy transfer in a lined hard- or soft-walled duct. Both of the above investigations were primarily concerned with nonlinear effects on attenuation of a fundamental wave.

⁷A.H. Nayfeh and M. Tsai, "Nonlinear Acoustic Propagation in Two-Dimensional Ducts," Journal of the Acoustical Society of America, 55 (1974), 1166-1172.

⁸A.H. Nayfeh, Perturbation Methods (New York: Wiley-Interscience, 1973), Chapter 6.

⁹P.G. Vaidya and K.S. Wang, "Nonlinear Propagation of Complex Sound Fields in Rectangular Ducts, Part I: The Self-Excitation Phenomenon," Journal of Sound and Vibration, 50 (1977), 29-42.

Acoustic parametric amplification has been suggested by Ostrovskii and Papilova,¹⁰ who investigated the amplification of a fundamental wave in an acoustic waveguide by injecting the second harmonic and utilizing the dispersivity of the guide to prevent higher-order interactions. This work was again limited to rigid or free boundaries.

For linear sound propagation, directivity enhancement of a conventional circular aperture transducer via an acoustic slow waveguide (e.g., silicone rubber immersed in water) has been observed experimentally by Rogers and Trott¹¹ and investigated numerically by King.¹²

Ryder, Rogers, and Jarzynski¹³ experimentally and numerically investigated the radiation of a nonlinearly generated difference frequency in a silicone rubber cylinder of finite length. However, their results are so completely

¹⁰L.A. Ostrovskii and I.A. Papilova, "Nonlinear Mode Interaction and Parametric Amplification in Acoustic Waveguides," Soviet Physics-Acoustics, 19 (1973), 45-50.

¹¹P.H. Rogers and W.J. Trott, "Acoustic Slow Waveguide Antenna," Journal of the Acoustical Society of America, 56 (1974), 1111-1117.

¹²B.J. King, "Numerical Investigation of an Acoustic Slow Waveguide," Journal of the Acoustical Society of America, 62 (1977), 1389-1396.

¹³J.D. Ryder, P.H. Rogers, and J. Jarzynski, "Radiation of Difference-Frequency Sound Generated by Nonlinear Interaction in a Silicone Rubber Cylinder," Journal of the Acoustical Society of America, 59 (1976), 1077-1086.

dependent on numerical analysis that no phenomenological predictions can be based on it.

1.5 Outline of the Analytical Approach

To derive Green's functions for the problem under consideration, the linear response of a three-layered medium to a sinusoidal point source of unit strength in medium II is deduced. The solutions thus obtained which are expressed in wavenumber space are then transformed into frequency space via complex integration techniques. The exact integral includes contributions from complex as well as real poles. However, as discussed in Chapter II, only real poles, which represent trapped energy, are considered. It is these discrete values of the axial wavenumber that define the dispersion of the waveguide for guided modes.

Distortion due to nonlinear wave interactions in the medium is represented by second-order terms of the acoustic wave equation given in Chapter III. For "weak" interactions, these second-order terms combine to form a forcing function which may be treated as a source distribution. The analytical form of the source distribution is convolved with the Green's functions to yield the sum- or difference-frequency velocity potential in medium II for guided modes.

Finally, making use of the derived solution, various characteristics of the nonlinearly generated sum and difference frequencies are investigated via computer graphics techniques as outlined in Chapter IV.

Chapter II

GREEN'S FUNCTIONS

2.1 Definition

In general, the Green's function represents the solution of a partial differential equation for a harmonic source of unit strength satisfying specified boundary conditions. As stated in the introduction, the behavior of free, dilatational waves in an acoustic medium is governed by the Helmholtz equation

$$(2-1) \quad (\nabla^2 + k^2)\phi_\omega = 0 \quad ,$$

where ϕ_ω represents the velocity potential in the frequency domain. Consider a point source of unit strength at a point (x', z') in medium II (i.e., $0 \leq x' \leq a$, $0 \leq z'$) oscillating with the same frequency as above. The governing equation describing the acoustic field at (x, z) in medium II is given by

$$(2-2) \quad (\nabla^2 + k^2) G_\omega(x, z | x', z') = -\delta(x-x')\delta(z-z') \quad ,$$

where $G_{\omega}(x, z | x', z')$ represents the Green's function and the Dirac delta functions on the right-hand side are defined to be zero everywhere except at the point $x=x'$, $z=z'$ where the amplitude becomes infinite but the magnitude (or the area under the curve) is unity. Mathematically, this can be expressed by the Dirac delta function:

$$(2-3) \quad \begin{array}{l} \text{a) } \delta(x) = 0 \quad x \neq 0 \\ \text{b) } \int_{-\infty}^{\infty} \delta(x) dx = 1 \end{array}$$

Likewise, it can be shown that;

$$(2-4) \quad \int_{-\infty}^{\infty} f(x) \delta(x) dx = f(0)$$

The Green's function $G_{\omega}(x, z | x', z')$ can thus be thought of as the normalized response at an observation point (x, z) to a point source of unit strength at (x', z') . It is then obvious from Equation (2-2) that the Green's function will be independent of a particular source distribution since the right-hand side of Equation (2-2) represents a point source.

2.2 Velocity Potential in Terms of Green's Functions

If a volume source distribution $S_{\omega}(x, z)$ at frequency ω exists in medium II, the wave equation assumes the inhomogeneous form

$$(2-5) \quad (\nabla^2 + k^2)\phi_\omega(x, z) = -S_\omega(x, z) \quad .$$

From the theory of linear differential operators, the solution of Equation (2-5) in the guide is given by the convolution of G_ω and S_ω :¹⁴

$$(2-6) \quad \phi_\omega(x, z) = \int_0^z \int_0^a S_\omega(x', z') G_\omega(x, z | x', z') dx' dz' \quad .$$

The above solution is valid for guided modes only, which are discussed later in the chapter.

The power and versatility of utilizing Green's functions may be seen in the above equation. Once $G_\omega(x, z | x', z')$ has been determined for a particular medium with specified boundary conditions; then, the response to any source distribution may be obtained via convolution. During the remainder of this chapter, expressions for $G_\omega(x, z | x', z')$ will be derived.

The first step in the analysis is to transform $G_\omega(x, z | x', z')$ into wavenumber space. In this manner, Equation (2-2) becomes an ordinary differential equation rather than a partial differential equation. The method of separation-of-the-variables then yields the assumed form for the transformed Green's function, the coefficients of which are obtained by matrix inversion (or, in this instance, via

¹⁴C. Lanczos, Linear Differential Operators (London: D. Van Nostrand Co. Ltd., 1961), pp. 206-314.

Cramer's rule). An inverse transformation from wavenumber space to real space, achieved via residue theory, then gives the Green's function for medium II.

2.3 Derivation of G_{χ}

As stated above, the Green's function satisfies the following equation:

$$(2-7) \quad \left(\frac{d^2}{dx^2} + \kappa^2\right) G_{\chi} = -\delta(x-x')\exp(-i\chi z') \quad ,$$

where

$$(2-8) \quad G_{\chi} = G_{\chi}(x|x',z') = \int_{-\infty}^{\infty} G_{\omega}(x,z|x',z')\exp(-i\chi z) dz \quad .$$

Equation (2-7) is a one-dimensional wave equation to which the following boundary conditions characteristic of a fluid-fluid interface are applied:

- a) continuity of pressure at $x=0, a, x'$
- b) continuity of normal velocity at $x=0, a$
- c) discontinuity of normal velocity at $x=x'$.

Since Equation (2-7) is homogeneous everywhere except at $x=x'$, then G_{χ} may be treated as a velocity potential. Hence, the boundary conditions become:

$$\begin{aligned}
 & \text{a) } \rho_i \frac{\partial G_{\chi_i}}{\partial t} = \rho_j \frac{\partial G_{\chi_j}}{\partial t} \quad ; \quad \text{at } x=0, a, x' \text{ for } i, j=1, 2, 3 \\
 (2-9) \quad & \text{b) } \frac{\partial G_{\chi_i}}{\partial x} = \frac{\partial G_{\chi_j}}{\partial x} \quad ; \quad \text{at } x=0, a \text{ for } i, j=1, 2, 3 \\
 & \text{c) } \lim_{\zeta \rightarrow 0} \frac{\partial G_{\chi}}{\partial x} \Bigg|_{x'-\zeta}^{x'+\zeta} = -\exp(-i\chi z') \quad ,
 \end{aligned}$$

where ρ_i is density in medium "i". The discontinuity at x' implied in condition (c) is a consequence of the nature of a point source. It is assumed that the point source lies in medium II (i.e., $0 \leq x' \leq a$ and $0 \leq z'$). Due to the infinite extent of the media along the z-axis, plane waves are assumed to propagate in the positive z-direction since no reflected (i.e., backward-going) waves are admitted. In the transverse direction, energy in medium II is reflected at the interfaces producing standing waves which are represented as interfering plane waves propagating in the positive and negative x-direction. Energy escaping into the semi-infinite surrounding media propagates away from the z-axis. The appropriate algebraic sign is chosen to describe waves which decay to zero at $x = \pm \infty$. The free-space wavenumber may be decomposed into its horizontal and vertical components using the following relationship:

$$(2-10) \quad k_i = \frac{\omega}{c_i} = \sqrt{\kappa_i^2 + \chi_i^2} \quad ,$$

where

κ_i = transverse wavenumber in medium "i",

and χ_i = axial wavenumber in medium "i" .

Applying the method of separation-of-the-variables to evaluate Equation (2-7) in the various regions defined in Figure 3 produces the following solutions:

$$(2-11) \quad \text{a) } x \geq a : G_{\chi} = A_1 \exp(i\kappa_1 x)$$

$$\text{b) } a \geq x \geq x' : G_{\chi} = B_1 \exp(i\kappa_2 x) + B_2 \exp(-i\kappa_2 x)$$

$$\text{c) } x' \geq x \geq 0 : G_{\chi} = C_1 \exp(i\kappa_2 x) + C_2 \exp(-i\kappa_2 x)$$

$$\text{d) } 0 \geq x : G_{\chi} = D_2 \exp(-i\kappa_3 x) \quad ,$$

where the coefficients A_1 , B_1 , B_2 , C_1 , C_2 , and D_2 depend on physical properties of the media. As stated above, the sign convention for the exponents in G_{χ} is chosen to avoid sources at $x = \pm \infty$, assuming harmonic time dependence $\exp(-i\omega t)$. It should also be noted, that in order to preserve continuity of the wavefront across the boundaries, the axial wavenumbers, χ_i , must be the same for all three media:

$$(2-12) \quad \chi_1 = \chi_2 = \chi_3 = \chi \quad .$$

Applying the boundary conditions given in Equation (2-9) to the above system yields a set of six linear equations:

$$a) \quad \rho_1 A_1 \exp(i\kappa_1 a) = \rho_2 B_1 \exp(i\kappa_2 a) + \rho_2 B_2 \exp(-i\kappa_2 a) \quad ,$$

$$b) \quad \rho_2 B_1 \exp(i\kappa_2 x') + \rho_2 B_2 \exp(-i\kappa_2 x') = \rho_2 C_1 \exp(i\kappa_2 x') + \rho_2 C_2 \exp(-i\kappa_2 x') \quad ,$$

$$c) \quad \rho_2 C_1 + \rho_2 C_2 = \rho_3 D_2 \quad ,$$

$$(2-13) \quad d) \quad \kappa_1 A_1 \exp(i\kappa_1 a) = \kappa_2 B_1 \exp(i\kappa_2 a) - \kappa_2 B_2 \exp(-i\kappa_2 a) \quad ,$$

$$e) \quad i\kappa_2 C_1 - i\kappa_2 C_2 = -i\kappa_3 D_2 \quad , \text{ and}$$

$$f) \quad -i\kappa_2 B_1 \exp(i\kappa_2 x') + i\kappa_2 B_2 \exp(-i\kappa_2 x') + i\kappa_2 C_1 \exp(i\kappa_2 x') - i\kappa_2 C_2 \exp(-i\kappa_2 x') = \exp(-i\chi z') \quad .$$

The solution may be obtained via Cramer's rule as applied to the matrix equation shown on the next page [Equation (2-14)].

$$\begin{bmatrix}
 \rho_1 \exp(i\kappa_1 a) - \rho_2 \exp(i\kappa_2 a) - \rho_2 \exp(-i\kappa_2 a) & 0 & 0 & 0 & 0 \\
 0 & \exp(i\kappa_2 x') & \exp(-i\kappa_2 x') & -\exp(i\kappa_2 x') & -\exp(-i\kappa_2 x') & 0 \\
 0 & 0 & 0 & \rho_2 & \rho_2 & -\rho_3 \\
 \kappa_1 \exp(i\kappa_1 a) & -\kappa_2 \exp(i\kappa_2 a) & \kappa_2 \exp(-i\kappa_2 a) & 0 & 0 & 0 \\
 0 & 0 & 0 & \kappa_2 & \kappa_2 & -\kappa_2 \\
 0 & -i\kappa_2 \exp(i\kappa_2 x') & i\kappa_2 \exp(-i\kappa_2 x') & i\kappa_2 \exp(i\kappa_2 x') & -i\kappa_2 \exp(-i\kappa_2 x') & 0
 \end{bmatrix}
 \times
 \begin{bmatrix}
 A_1 \\
 B_1 \\
 B_2 \\
 C_1 \\
 C_2 \\
 D_2
 \end{bmatrix}
 =
 \begin{bmatrix}
 0 \\
 0 \\
 0 \\
 0 \\
 0 \\
 \exp(-i\kappa_2 a)
 \end{bmatrix}$$

Equation (2-14)

Expressions for the six coefficients A_1 , B_1 , B_2 , C_1 , C_2 , and D_2 involve a ratio of sixth-order determinants. A computer program named SYMLEQ (PSU Computation Center) performs the algebraic manipulations required for the solution of the matrix equation $AX=B$, where elements of the matrices A and B may be algebraic symbols or numeric constants. A discussion of the algorithm and general guidelines for the use of SYMLEQ are given in a PSU program guide.¹⁵ Solving Equation (2-14) (via SYMLEQ) for A_1 , B_1 , B_2 , C_1 , C_2 , and D_2 and substituting into Equation (2-11) leads to the following expressions for G_X in each region of the transverse plane:

Region I, $x \geq a$:

$$(2-15) \quad G_X = 2\exp(-i\chi z')\exp(i\kappa_1(x-a)) \frac{[\text{Exp}(i\kappa_2 x') - \text{Fexp}(-i\kappa_2 x')]}{4\kappa_2 \Psi(\chi)}$$

¹⁵H.D. Knoble, "Solution of Simultaneous Linear Equations Involving Matrices Whose Elements are Symbolic Multivariate (Complex) Polynomials" (Program user's guide, The Pennsylvania State University Computation Center, 1971).

Region IIA, $a > x > x'$:

$$(2-16) \quad G_x = \exp(-i\chi z') \frac{[A \exp(-i\kappa_2(x-a)) + B \exp(i\kappa_2(x-a))] \exp(i\kappa_2 x') + [C \exp(-i\kappa_2(x-a)) + D \exp(i\kappa_2(x-a))] \exp(-i\kappa_2 x')}{4\kappa_2 \Psi(\chi)}$$

Region IIB, $x' > x > 0$:

$$(2-17) \quad G_x = \exp(-i\chi z') \frac{\{ [A \exp(-i\kappa_2(x'-a)) + B \exp(i\kappa_2(x'-a))] \exp(i\kappa_2 x) + [C \exp(-i\kappa_2(x'-a)) + D \exp(i\kappa_2(x'-a))] \exp(-i\kappa_2 x) \}}{4\kappa_2 \Psi(\chi)}$$

Region III, $x < 0$:

$$(2-18) \quad G_x = 2 \exp(-i\chi z') \exp(-i\kappa_3 x) \frac{[G \exp(-i\kappa_2(x'-a)) - H \exp(i\kappa_2(x'-a))]}{4\kappa_2 \Psi(\chi)}$$

where the following substitutions have been made in order to simplify the functional form of the coefficients:

Let

$$\begin{aligned}
 (2-19) \quad a &= \rho_2^3 \kappa_1 \kappa_3 & e &= \rho_2^3 \kappa_2 \kappa_3 \\
 b &= \rho_1 \rho_2^2 \kappa_2 \kappa_3 & f &= \rho_2^2 \rho_3 \kappa_2^2 \\
 c &= \rho_2^2 \rho_3 \kappa_1 \kappa_2 & g &= \rho_2^3 \kappa_1 \kappa_2 \\
 d &= \rho_1 \rho_2 \rho_3 \kappa_2^2 & h &= \rho_1 \rho_2^2 \kappa_2^2
 \end{aligned}$$

Then

$$\begin{aligned}
 A &= -a+b+c-d & E &= e-f \\
 B &= a+b-c-d & F &= e+f \\
 (2-20) \quad C &= a-b+c-d & G &= g-h \\
 D &= -a-b-c-d & H &= g+h
 \end{aligned}$$

Hence, the function $\Psi(\chi)$ is given by:

$$\begin{aligned}
 (2-21) \quad \Psi(\chi) &= (i/2)(A \exp(i\kappa_2 a) - D \exp(-i\kappa_2 a)) \\
 &= (a+d) \sin(\kappa_2 a) + i(b+c) \cos(\kappa_2 a)
 \end{aligned}$$

Note that when 'a' occurs in the exponent, it refers to the thickness of the waveguide, not the variable in Equations (2-19) and (2-20).

Notice that Equations (2-15)-(2-18) represent the transformed Green's functions for medium II since it was assumed that $0 < x' \leq a$. Green's functions for media I and III have been similarly derived and are given in Appendix C. Equations (2-15)-(2-18) are in agreement with previously published work in the field of optics if it is assumed that $\rho_1 = \rho_2 = \rho_3 = 1$.¹⁶

2.4 Inverse Transformation of G_χ

The Green's functions in the frequency domain $G_\omega(x, z | x', z')$ are now found by taking the inverse Fourier transform of G_χ :

$$(2-22) \quad G_\omega(x, z | x', z') = \frac{1}{2\pi} \int_{-\infty}^{\infty} G_\chi(x | x', z') \exp(i\chi z) d\chi$$

Due to the complex nature of χ , the integration extends over the entire complex plane. The residue of G_χ at all of its poles must be determined in order to evaluate Equation (2-22) via Cauchy's Residue Theorem. However, as will be discussed, the contributions from certain poles are neglected.

The poles of G_χ form a discrete spectrum of values of the axial wavenumber χ . Real poles are associated with propagating modes. It is these modes which transport most of the energy through the waveguide. Complex poles give rise to leaky wave modes which are more thoroughly discussed by Kapany and Burke,¹⁷ and by Marcuse.¹⁸ Leaky modes are

¹⁶C.C. Ghizoni, J.M. Ballantyne and C.L. Tang, "Theory of Optical-Waveguide Distributed Feedback Lasers: A Green's Functions Approach," IEEE Journal of Quantum Electronics, 13 (1977), 843-848.

¹⁷N.S. Kapany and J.J. Burke, Optical Waveguides, (New York: Academic Press, 1972), pp. 24-34.

¹⁸D. Marcuse, Theory of Dielectric Optical Waveguides, (New York: Academic Press, 1974), pp. 41-46.

those which continually radiate power from the guide as they propagate down the duct thus being rapidly attenuated. Finally, in the extreme case, imaginary poles represent evanescent modes whose amplitudes decrease exponentially with range. The effects of evanescent modes and leaky wave modes are thus confined to ranges very near the source. Hence, considering only propagating modes (or those for which χ is real) and ignoring nearfield effects permits the integral [Equation (2-22)] to be approximated as a sum of residues of poles on the real axes only.

The real, axial wavenumber χ may range anywhere from zero to infinity for each frequency. Since it is assumed that $c_3 \geq c_1 > c_2$, then the free-space wavenumbers are related by $k_3 \leq k_1 < k_2$. Also, from Equation (2-10), the magnitude of the transverse wavenumber in medium 'i' is given by:

$$(2-23) \quad \kappa_i = \sqrt{k_i^2 - \chi^2} \quad ; \quad i=1,2,3 \quad .$$

For χ in the range $0 \leq \chi \leq k_3$, all transverse wavenumbers κ_i are real and it can readily be seen from Equation (2-11) that this represents a radiation mode. For χ in the range $k_3 \leq \chi \leq k_1$, the transverse wavenumbers κ_1 and κ_2 are real, whereas κ_3 is pure imaginary. Hence, this mode, which is confined to media I and II with energy decaying exponentially in medium III, is therefore called a substrate mode. For $k_1 \leq \chi \leq k_2$, as seen from Equation (2-23), κ_1 and κ_3

are imaginary and κ_2 is real so that all energy propagating under these conditions is restricted to medium II, hence, the term guided mode. Propagation of guided modes is characterized by total internal reflection at both upper and lower interfaces. Finally, for $\chi > \kappa_2$, all transverse wavenumbers are imaginary so that no propagating wave can exist. The term evanescent mode is used to describe this condition under which all energy decays exponentially in the direction of wave propagation. Regions for each mode type are depicted in Figure 4 which shows the relationship between angular frequency ω and axial wavenumber χ .

2.5 Discussion of Poles of G_χ

In order to evaluate the integral defined by Equation (2-22), it is necessary to locate the poles of the integrand and evaluate the residues. Since $G_\chi = F(\chi)/\Psi(\chi)$ the roots of the equation $\Psi(\chi) = 0$ define the poles of G_χ . Setting the function $\Psi(\chi) = 0$ results in the following transcendental equation:

$$(2-24) \quad \tan(\kappa_2 a) = \frac{-i(\rho_2 \rho_3 \kappa_1 \kappa_2 + \rho_1 \rho_2 \kappa_2 \kappa_3)}{\rho_1 \rho_3 \kappa_2 + \rho_2 \kappa_1 \kappa_3}$$

where the transverse wavenumbers are given in Equation (2-23). Equation (2-24) has two possible solutions for real

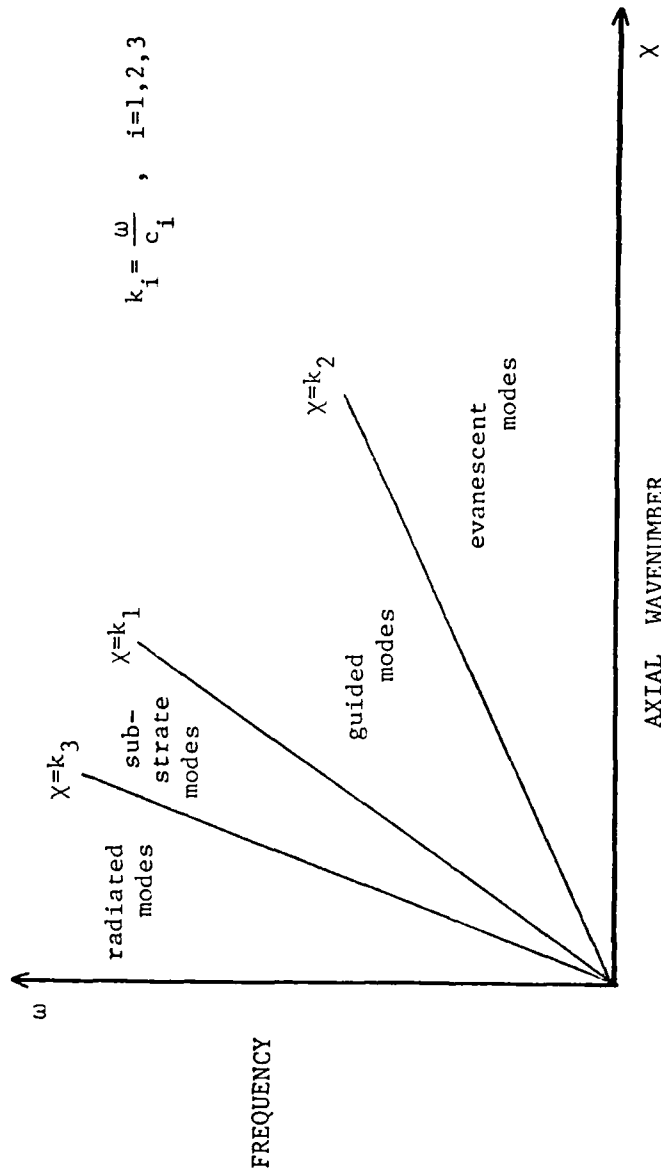


Figure 4. Modes of propagation in an acoustic waveguide for real axial wavenumber.

χ : either κ_1 , κ_2 and κ_3 are all pure imaginary, or κ_2 is real and κ_1 and κ_3 are imaginary. As discussed earlier, the former case does not permit a propagating wave to exist. Hence, for real χ , κ_1 and κ_3 are imaginary with κ_2 real; that is, χ is in the range $k_1 \leq \chi \leq k_2$. Under these conditions, only guided modes may propagate as previously discussed and shown in Figure 4. The transverse wavenumbers may be redefined to satisfy the above conditions:

$$(2-25) \quad \begin{aligned} \kappa_1 &= i\kappa_{1m} \\ \kappa_2 &= \kappa_{2m} \\ \kappa_3 &= i\kappa_{3m} \end{aligned} ,$$

where the subscript "m" denotes mode number as well as indicating a positive, real quantity. Depending on the magnitude of the argument of the tangent function (i.e., $\kappa_2 a$), Equation (2-24) has "m" roots for any given frequency, where the m^{th} pole, $\pm\chi_m$, satisfies the following transcendental equation obtained by substituting Equation (2-25) into Equation (2-24):

$$(2-26) \quad \tan(\kappa_{2m} a) = \frac{\rho_2 \rho_3 \kappa_{1m} \kappa_{2m} + \rho_1 \rho_2 \kappa_{2m} \kappa_{3m}}{\rho_1 \rho_3 \kappa_{2m} - \rho_2 \kappa_{1m} \kappa_{3m}} .$$

It is possible, when dealing with a ratio of functions, for a zero to cancel a pole and thus eliminate the apparent singularity. This is the case for one root of Equation (2-26); in particular $\chi_m = k_2$, which is discussed in Appendix B (see Plane-Wave Mode).

Now, the integrand of Equation (2-22) is more simply expressed in the following form:

$$(2-27) \quad G_{\omega}(x, z | x', z') = \frac{1}{2\pi} \int_{-\infty}^{\infty} G_{\chi}(x | x', z') \exp(i\chi z) d\chi$$

$$= \int_{-\infty}^{\infty} \frac{F(\chi)}{\Psi(\chi)} \exp(i(z-z')\chi) d\chi$$

where the function $F(\chi)$ may be deduced from expressions for G_{χ} given in Equations (2-15)-(2-18) and $\Psi(\chi)$ is defined in Equation (2-21).

2.6 Contour Integration

As previously stated, the poles of interest lie on the real axis. By convention, the time factor has been chosen to be $\exp(-i\omega t)$. Therefore, real poles greater than zero

correspond to waves propagating in the positive z -direction. All physical problems involve at least a small amount of damping which is accounted for by including an imaginary term, of appropriate algebraic sign, in the axial wavenumber. It is apparent that for waves propagating in the positive z -direction (i.e., for $z \geq z'$), the imaginary part of χ_m must be greater than zero to satisfy the condition that, as time increases, the amplitude will decrease to zero as $z \rightarrow \infty$. Similarly, for $z < z'$, the imaginary part must be less than zero. The inclusion of damping, therefore, shifts the positive poles into the upper half, and the negative poles into the lower half of the complex χ plane.

A section of the contour of integration for Equation (2-27) is depicted in Figure 5. Branch cuts must be made due to the multivalued functions involved (i.e., $\chi = \sqrt{k_2^2 - \kappa_2^2}$). Contributions to the integral along these cuts have been neglected for the current investigation. To obtain exponential decay of the semicircular contribution to Equation (2-27), the following must be true:

$$(2-28) \quad \lim_{|\chi| \rightarrow 0} |\exp(i(z-z')\chi)| = 0 .$$

This says that the path of integration in the upper half plane applies to $z \geq z'$ and includes the poles χ_m greater than

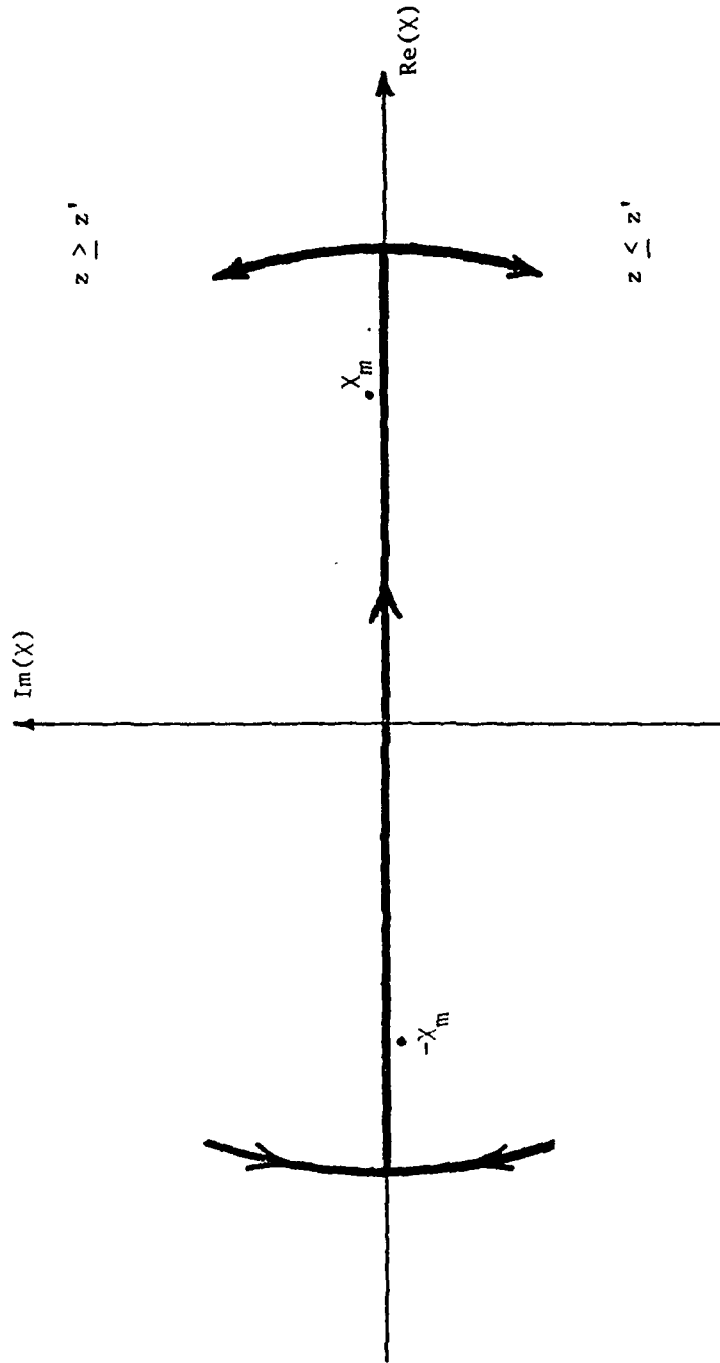


Figure 5. Contour integration in complex axial wavenumber (X) plane around the poles $\pm X_m$ for $z < \underline{z'}$ and $z > \underline{z'}$.

zero. Then, by Cauchy's Residue Theorem, the Green's function G_ω [Equation (2-27)] for forward-guided modes is given by a sum of residues at the positive real poles χ_m :

$$\begin{aligned}
 (2-29) \quad G_\omega(x, z | x', z') &= \frac{1}{2\pi} \int_{-\infty}^{\infty} G_\chi \exp(i\chi z) d\chi \\
 &= 2\pi i \sum_{m=1}^{\infty} \text{RES} \left[\frac{G_\chi \exp(i\chi z)}{2\pi}; \chi = \chi_m > 0 \right] \\
 &= \sum_{m=1}^{\infty} G_m^+ ,
 \end{aligned}$$

where G_m^+ represents the Green's function for the m^{th} forward-guided mode.

2.7 Evaluation of Residues

The residue of a quotient of functions which has a first order pole at $\chi = \chi_m$ is given by:

$$(2-30) \quad \text{RES} \left[\frac{F(\chi)}{\Psi(\chi)}; \chi = \chi_m \right] = \lim_{\chi \rightarrow \chi_m} \left[\frac{F(\chi)}{\Psi'(\chi)} \right] ,$$

where $\Psi'(\chi_m)$ has been differentiated with respect to χ . Expressions for G_m^+ are obtained via Equations (2-30) and

(2-29) together with Equations (2-15)-(2-22) which originally defined G_χ .

Region I, $x \geq a$:

$$(2-31) \quad G_m^+ = 2i \exp(i\chi_m(z-z')) \exp(-\kappa_{1m}(x-a)) \frac{[E_m \exp(i\kappa_{2m}x') - F_m \exp(-i\kappa_{2m}x')]}{4\kappa_{2m}\psi'(\chi_m)}$$

Region IIA, $a \geq x \geq x'$

$$(2-32) \quad G_m^+ = i \exp(i\chi_m(z-z')) \left\{ \frac{[A_m \exp(-i\kappa_{2m}(x-a))]}{4\kappa_{2m}\psi'(\chi_m)} + \frac{B_m \exp(i\kappa_{2m}(x-a)) \exp(i\kappa_{2m}x') + [C_m \exp(-i\kappa_{2m}(x-a))]}{4\kappa_{2m}\psi'(\chi_m)} + \frac{D_m \exp(i\kappa_{2m}(x-a)) \exp(-i\kappa_{2m}x')}{4\kappa_{2m}\psi'(\chi_m)} \right\}$$

Region IIB, $x' \geq x \geq 0$

$$(2-33) \quad G_m^+ = i \exp(i\chi_m(z-z')) \left\{ \frac{[A_m \exp(-i\kappa_{2m}(x'-a))]}{4\kappa_{2m}\psi'(\chi_m)} + \frac{B_m \exp(i\kappa_{2m}(x'-a)) \exp(i\kappa_{2m}x) + [C_m \exp(-i\kappa_{2m}(x'-a))]}{4\kappa_{2m}\psi'(\chi_m)} + \frac{D_m \exp(i\kappa_{2m}(x'-a)) \exp(-i\kappa_{2m}x)}{4\kappa_{2m}\psi'(\chi_m)} \right\}$$

Region III, $x \leq 0$

$$(2-34) \quad G_m^+ = 2i \exp(i\chi_m(z-z')) \exp(\kappa_{3m}x) \frac{[G_m \exp(-i\kappa_{2m}(x'-a))]}{4\kappa_{2m}\psi'(\chi_m)} - \frac{H_m \exp(i\kappa_{2m}(x'-a))}{4\kappa_{2m}\psi'(\chi_m)}$$

where the following expressions are obtained by substituting Equation (2-25) into Equations (2-19) and (2-20):

Let

$$(2-35) \quad \begin{aligned} a_m &= -\rho_2^3 \kappa_{1m} \kappa_{3m} & e_m &= i\rho_2^3 \kappa_{2m} \kappa_{3m} \\ b_m &= i\rho_1 \rho_2^2 \kappa_{2m} \kappa_{3m} & f_m &= \rho_2^2 \rho_3 \kappa_{2m}^2 \\ c_m &= i\rho_2^2 \rho_3 \kappa_{1m} \kappa_{2m} & g_m &= i\rho_2^3 \kappa_{1m} \kappa_{2m} \\ d_m &= \rho_1 \rho_2 \rho_3 \kappa_{2m}^2 & h_m &= \rho_1 \rho_2^2 \kappa_{2m}^2 \end{aligned}$$

Then,

$$(2-36) \quad \begin{aligned} A_m &= -a_m + b_m + c_m - d_m & \text{and} & & E_m &= e_m - f_m \\ B_m &= a_m + b_m - c_m - d_m & & & F_m &= e_m + f_m \\ C_m &= a_m - b_m + c_m - d_m & & & G_m &= g_m - h_m \\ D_m &= -a_m - b_m - c_m - d_m & & & H_m &= g_m + h_m \end{aligned}$$

where

$$(2-37) \quad \begin{aligned} \kappa_{1m} &= \sqrt{\chi_m^2 - k_1^2} \\ \kappa_{2m} &= \sqrt{k_2^2 - \chi_m^2} \\ \kappa_{3m} &= \sqrt{\chi_m^2 - k_3^2} \end{aligned}$$

The expression for $\Psi'(\chi_m)$ is derived in Appendix A, the results of which are restated here:

$$\begin{aligned}
 (2-38) \quad \Psi'(\pm\chi_m) &= \left. \frac{\partial \Psi(x)}{\partial x} \right|_{x=\pm\chi_m} \\
 &= (\pm\chi_m) \left[(\rho_2^3 \frac{\kappa_{1m}^2 + \kappa_{3m}^2}{\kappa_{1m} \kappa_{3m}} + 2\rho_1 \rho_2 \rho_3 + \rho_2^2 \rho_3 \kappa_{1m} a + \right. \\
 &\quad \left. \rho_1 \rho_2^2 \kappa_{3m} a) \sin(\kappa_{2m} a) + (\rho_1 \rho_2 \rho_3 \kappa_{2m} a + \rho_2^2 \rho_3 \frac{\kappa_{2m}}{\kappa_{1m}} - \right. \\
 &\quad \left. \frac{(\rho_2^2 \rho_3 \kappa_{1m} + \rho_2^3 \kappa_{1m} \kappa_{3m} a + \rho_1 \rho_2^2 \kappa_{3m})}{\kappa_{2m}} + \rho_1 \rho_2^2 \frac{\kappa_{2m}}{\kappa_{3m}}) \cos(\kappa_{2m} a) \right]
 \end{aligned}$$

By inspection, it can be seen that, for $x=x'$, G_m^+ in region IIA is equal to G_m^+ in region IIB.

2.8 Boundary-Induced Dispersion

It is evident from the form of Equation (2-29) that the Green's function is expressed as an eigenfunction expansion of guided modes where the poles of $G_\chi(x|x',z')$, namely χ_m , are also eigenvalues of the system. Numerical methods used to evaluate these eigenvalues will be discussed in Chapter IV.

Once the physical parameters of the system are known (i.e., density and bulk phase velocity of media I, II, and III and thickness of medium II), the variation of axial wavenumber χ_m with frequency for each mode may be determined. For example, Figure 6 shows frequency as a

function of axial wavenumber for the first few modes of an infinite flat-plate of silicone rubber 10 centimeters thick immersed in water.

Several aspects of this graph will be discussed later in Chapter IV. However, one important point should be made at this time. In a nondispersive medium, that is one in which phase velocity is independent of frequency, wavenumber and frequency are linearly related. Figure 6 illustrates the fact that for any given mode, low-frequency disturbances tend to propagate at the higher phase velocity of the external media (i.e., I and III). Contrariwise, the speed of higher frequency components asymptotically approaches that of the waveguide (medium II). This phenomenon is referred to as "boundary-induced dispersion" and will be discussed in greater detail in Chapter IV.

MEDIUM	PHASE VEL.*	DENSITY*	THICKNESS*	MODE	CUTOFF (kHz)
I	1500.0	1000.0	∞	1	0.00
II	1000.0	1000.0	0.10	2	6.70
III	1500.0	1000.0	∞	3	13.41

* SI UNITS

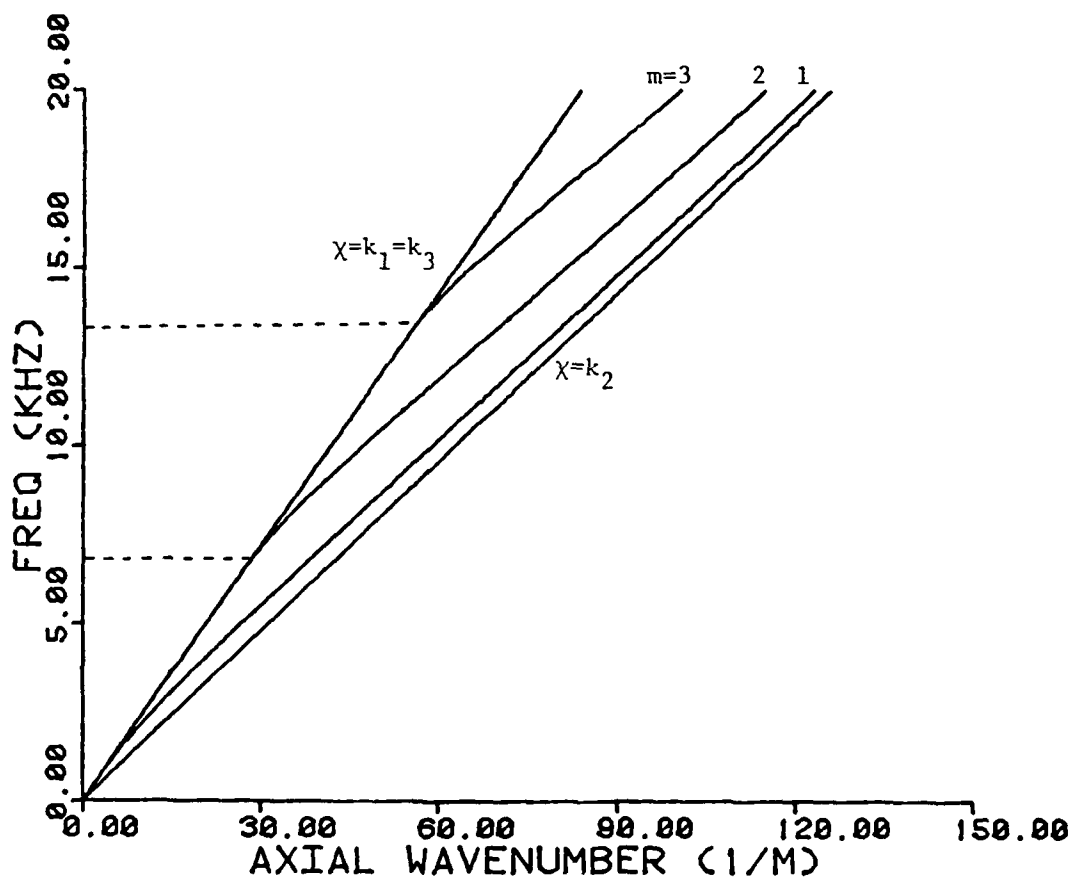


Figure 6. Dispersion relationship for first few guided modes in a 0.1 m.-thick slab of silicone rubber immersed in water. Isospeed lines at $\chi = k_1, k_2$ represent bounds for trapped energy. Dashed lines indicate cutoff frequencies for modes $m=2, 3$.

Chapter III

NONLINEAR WAVE INTERACTIONS IN LAYERED MEDIA

3.1 Introduction

The homogeneous wave Equation (2-1) is a linear, partial differential equation obtained by neglecting all terms of second- or higher-order. If, however, convective and medium nonlinearities are taken into consideration, inclusion of second-order terms leads to the following nonlinear wave equation, where viscoelastic and other loss mechanisms have been neglected:

$$(3-1) \quad \left(\frac{\partial^2}{\partial t^2} - c_0^2 \nabla^2 \right) \phi = \frac{-\partial}{\partial t} [|\tilde{\nabla} \phi|^2] + \frac{\gamma-1}{2c_0^2} \left(\frac{\partial \phi}{\partial t} \right)^2$$

with

γ = ratio of specific heat in gases ($1 + \frac{B}{A}$ in liquids)¹⁹

ϕ = the velocity potential.

¹⁹R.T. Beyer, "Parameter of Nonlinearity in Fluids," Journal of the Acoustical Society of America, 9 (1960), 719-721.

Equation (3-1) is the second-order, nonlinear wave equation. The source term, or right-hand side of this equation, contains the square of first-order acoustic fields. Hence, an originally monotonic sound field will result in a second-harmonic source term over distances which are considerably smaller than the critical range at which shock formation occurs. The new field, no longer being monotonic, is again squared over the next incremental distance giving rise to interaction between the fundamental and second harmonic, which in turn produces a third-harmonic field component. In an inviscid medium, this continuous process eventually leads to the formation of a shock wave, the spectrum of which contains all harmonics of the fundamental.

Similarly, bifrequency excitation leads not only to the generation of harmonics of each primary frequency, but also to intermodulation frequency components which result from interaction between the primary fields. Hence, the principle of linear superposition no longer holds. Of particular interest are the sum and difference frequencies (denoted by $\omega_{\pm} = \omega_1 \pm \omega_2$, for $\omega_1 > \omega_2$).

In general, various loss mechanisms inhibit the formation of weak shock waves in viscoelastic fluids. Such loss mechanisms are included via complex wavenumbers in the current investigation. It is assumed that the nonlinear interaction is weak enough to allow the velocity potential

on the right-hand side of Equation (3-1) to be approximated by a linear superposition of the primary fields. This approximation, commonly made in weak finite-amplitude acoustics, has been more thoroughly discussed by Fenlon.²⁰

Using the following Fourier transform relationship,

$$(3-2) \quad \phi(x, z, t) = \int_{-\infty}^{\infty} \phi_{\omega}(x, z) \exp(-i\omega t) d\omega, \quad ,$$

where

$$(3-3) \quad \phi_{\omega}(x, z) = \frac{1}{2\pi} \int_{-\infty}^{\infty} \phi(x, z, t) \exp(i\omega t) dt, \quad ,$$

the primary fields can then be expressed via the eigenmode expansion at the two frequencies ω_1 and ω_2 :

$$(3-4) \quad \phi_{\omega_1}(x, z) = \sum_{q=-\infty}^{\infty} C_q^{\omega_1} \exp(i(\chi_q^{\omega_1} z + \kappa_q^{\omega_1} x))$$

$$(3-5) \quad \phi_{\omega_2}(x, z) = \sum_{s=-\infty}^{\infty} C_s^{\omega_2} \exp(i(\chi_s^{\omega_2} z + \kappa_s^{\omega_2} x)).$$

Thus for weak, bifrequency wave interactions in medium II, if Equation (3-2) is substituted into Equation (3-1), and only those terms involved in sum- or difference-frequency

²⁰F.H. Fenlon, "On the Performance of a Dual Frequency Parametric Source Via Matched Asymptotic Solutions of Burgers' Equation," Journal of the Acoustical Society of America, 55 (1974), 35-46.

generation are retained, the resulting inhomogeneous Helmholtz equation at these frequencies is given by:

$$(3-6) \quad (\nabla^2 + k_{\pm}^2) \phi_{\omega_{\pm}} = \frac{i\omega_{\pm}}{c_2} \left[\bar{\nabla} \phi_{\omega_1} \cdot \bar{\nabla} \phi_{\omega_2}^{(*)} + \left(\frac{\gamma-1}{2} \right) k_1 k_2 \phi_{\omega_1} \phi_{\omega_2}^{(*)} \right],$$

where ϕ_{ω_i} represents the "linearized" velocity potential in medium II, and k_i represents the free-space wavenumbers in medium II for primary frequency ω_i , ω_{\pm} being the sum or difference frequency (i.e., $\omega_{\pm} = \omega_1 \pm \omega_2$).²¹ The superscript "*" in parentheses which appears in the velocity potential in Equation (3-6) implies that the complex conjugate only applies to the difference frequency.

That is,

$$\phi_{\omega_2}^{(*)} = \phi_{\omega_2} \quad \text{for } S_{\omega_+}(x,z)$$

and

$$\phi_{\omega_2}^{(*)} = \phi_{\omega_2}^* \quad \text{for } S_{\omega_-}(x,z).$$

3.2 Frequency-Domain Solution

The second-order, nonlinear wave equation in the frequency domain is given by Equation (3-6). It may be seen, by comparing this equation with the general form of

²¹F.H. Fenlon, private communication, October 17, 1979.

the inhomogeneous Helmholtz equation given in Equation (2-5), that the nonlinear terms which are grouped on the right-hand side of the equation can be thought of as a forcing function, or volume source distribution in the guide. This being the case, the velocity potential in medium II for a particular frequency is given by Equation (2-6):

$$(2-6) \quad \phi_{\omega}(x, z) = \int_0^z \int_0^a S_{\omega}(x', z') G_{\omega}(x, z | x', z') dx' dz' .$$

Hence, in order to evaluate Equation (2-6) for the sum- or difference-frequency component, the source distribution $S_{\omega_{\pm}}(x, z)$ must be determined. By inspection of Equation (3-6), the latter can be expressed as

$$(3-7) \quad S_{\omega_{\pm}}(x, z) = \frac{i\omega_{\pm}}{c_2} [\tilde{\nabla}\phi_{\omega_1} \cdot \tilde{\nabla}\phi_{\omega_2}^{(*)} + \left(\frac{\gamma-1}{2}\right) k_1 k_2 \phi_{\omega_1} \phi_{\omega_2}^{(*)}]$$

[see Equation (3-6) for definition of terms].

The first step in determining $\phi_{\omega_{\pm}}$ therefore, is to evaluate the source distribution in Equation (3-7). The next is to convolve the resulting function with the appropriate Green's function and perform the integration over x' and z' for a typical mode.

3.3 Source Distribution

The sum- or difference-frequency source distribution for weak finite-amplitude interaction in medium II is given in Equation (3-7).²² The primary waves are represented as eigenmode expansions [see Equation (3-6)] and hence, the scalar product of the primary velocity vectors is given by the double summation:

$$(3-8) \quad \bar{\nabla}\phi_{\omega_1} \cdot \bar{\nabla}\phi_{\omega_2}^{(*)} = \sum_{q,s=-\infty}^{\infty} \sum C_q^{\omega_1} C_s^{\omega_2} [\kappa_q^{\omega_1} \kappa_s^{\omega_2} + \chi_q^{\omega_1} \chi_s^{\omega_2}] \times \\ \exp\{i[(\chi_q^{\omega_1} \pm \chi_s^{\omega_2})z + (\kappa_q^{\omega_1} \pm \kappa_s^{\omega_2})x]\} .$$

Likewise, the product of the primary wave velocity potentials is simply

$$(3-9) \quad \phi_{\omega_1} \cdot \phi_{\omega_2}^{(*)} = \sum_{q,s=-\infty}^{\infty} \sum C_q^{\omega_1} C_s^{\omega_2} \exp\{i[(\chi_q^{\omega_1} \pm \chi_s^{\omega_2})z + (\kappa_q^{\omega_1} \pm \kappa_s^{\omega_2})x]\} .$$

Substituting Equations (3-8) and (3-9) into Equation (3-7) thus gives the following form for the sum- and difference-frequency source distribution at the source point (x', z') :

²²It is assumed that all nonlinear wave interactions occur within the guide (i.e., $0 < x \leq a$ and $z \geq 0$); therefore, the velocity potentials and wavenumbers for the primary fields correspond to medium II. With this in mind, the notation becomes slightly less laborious.

$$(3-10) \quad S_{\omega_{\pm}}(x', z') = \frac{i\omega_{\pm}}{c_2} \sum_{q, s=-\infty}^{\infty} C_q^{\omega_1} C_s^{\omega_2 (*)} [+(\chi_q^{\omega_1} \chi_s^{\omega_2} + \kappa_q^{\omega_1} \kappa_s^{\omega_2}) + (\frac{\gamma-1}{2})k_1 k_2] \times \\ \exp\{i[(\chi_q^{\omega_1} \pm \chi_s^{\omega_2})z' + (\kappa_q^{\omega_1} \pm \kappa_s^{\omega_2})x']\} \quad ,$$

where

$$\omega_{\pm} = \omega_1 \pm \omega_2$$

$$k_i = \omega_i / c_2 \quad (i=1,2)$$

$\kappa_q^{\omega_m}$ = transverse wavenumber for mode 'q',

frequency ω_m , medium II, $m=1,2$.

$\chi_q^{\omega_m}$ = axial wavenumber for mode 'q',

frequency ω_m , medium II, $m=1,2$.

$C_q^{\omega_m}$ = weighting coefficient for mode 'q',

frequency ω_m ; determined by actual source

distribution at face of waveguide (i.e., $z=0$)

γ = ratio of specific heat in gases ($1 + \frac{B}{A}$ in liquids).²³

Equation (3-10) defines the distribution of source points which contribute to the growth of the nonlinearly generated sum- and difference-frequency fields inside the waveguide. These points are referred to as "virtual" sources because they act as point sources scattered throughout the region of interaction generating the harmonic and intermodulation frequency components.²⁴

²³R.T. Beyer, "Parameter of Nonlinearity in Fluids," Journal of the Acoustical Society of America, 9 (1960), 719-721.

²⁴See e.g., H.O. Berktaay and C.A. Al-Temimi, "Virtual Arrays for Underwater Reception," Journal of Sound and

3.4 Evaluation of $\phi_{\omega_{\pm}}$

Recall that the Green's functions for forward-guided modes in each region are given by a sum of residues at real poles, which is analogous to an eigenmode expansion:

$$(2-29) \quad G_{\omega}(x, z | x', z') = \sum_{m=1}^{\infty} G_m^+$$

Expressions for G_m^+ are given in Chapter II [Equations (2-31)-(2-34)]. Multiplying the Green's functions for region IIA [Equation (2-32)] by the source distribution given by Equation (3-10) thus leads to the following expression for the velocity potential in medium II as per Equation (2-6):

$$(3-11) \quad \phi_{\omega_{\pm}}(x, z) = - \left(\frac{\omega_{\pm}}{4c_2^2} \right) \sum_{m=1}^{\infty} \sum_{q, s=-\infty}^{\infty} C_q^{\omega_1} C_s^{\omega_2} R X Z, \quad *$$

where

$$R = \frac{\left(\frac{\gamma-1}{2}\right) k_1 k_2 + (\chi_q^{\omega_1} \chi_s^{\omega_2} + \kappa_q^{\omega_1} \kappa_s^{\omega_2})}{\kappa_m^{\omega_{\pm}} \psi'(\chi_m^{\omega_{\pm}})},$$

$\kappa_m^{\omega_{\pm}}$ = transverse wavenumber in medium II (see text)
at frequency ω_{\pm} for mode m

and

(3-12) X = transverse component

$$= [A_m \exp(-i\kappa_m^{\omega_{\pm}}(x-a)) + B_m \exp(i\kappa_m^{\omega_{\pm}}(x-a))] \int_0^a \exp(i\Delta_x^+ x') dx' \\ + [C_m \exp(-i\kappa_m^{\omega_{\pm}}(x-a)) + D_m \exp(i\kappa_m^{\omega_{\pm}}(x-a))] \int_0^a \exp(i\Delta_x^- x') dx' ,$$

(3-13) Z = axial component

$$= \exp(i\chi_m^{\omega_{\pm}} z) \int_0^z \exp(i\Delta_z z') dz' ,$$

where

$$\Delta_x^+ = \kappa_q^{\omega_1} + \kappa_s^{\omega_2} + \kappa_m^{\omega_{\pm}}$$

$$\Delta_x^- = \kappa_q^{\omega_1} + \kappa_s^{\omega_2} - \kappa_m^{\omega_{\pm}}$$

$$\Delta_z = \chi_q^{\omega_1} + \chi_s^{\omega_2} - \chi_m^{\omega_{\pm}}$$

and A_m , B_m , C_m , D_m are all defined in Equation (2-36), $\Psi'(\chi_m^{\omega_{\pm}})$ being given by Equation (2-38).

The velocity potential is thus represented as a triple summation over m , q , and s , where m represents the mode in which the sum or difference frequency propagates, and q and s are the modes excited by the primary field sources ω_1 and ω_2 at $z=0$.

In order to examine the contribution of a particular set of modes, terms for positive and negative q and s should be included for each integer value of m , since waves travel in both the positive and negative x -directions inside the

guide. Therefore, for fixed values of m , q , and s , the x -component of Equation (3-11) involves two terms designated by a subscript (i.e., X_+ and X_-) to distinguish between q and s being greater or less than zero. Then since

$$(3-14) \quad \int_0^b \exp(iar) dr = b \exp(iab/2) \operatorname{sinc}(ab/2) ,$$

where $\operatorname{sinc}(x) = \sin(x)/x$, the transverse and axial components of Equation (3-11), i.e., Equations (3-12) and (3-13), become:

$$(3-15) \quad X_+ = (J+K) \exp(i\kappa_m^+ x) + (L+M) \exp(-i\kappa_m^+ x) ,$$

where

$$J = B_m a \operatorname{sinc}(\Delta_x^+ a/2) \exp(-i(\kappa_m^+ a - \Delta_x^+ a/2))$$

$$K = D_m a \operatorname{sinc}(\Delta_x^- a/2) \exp(-i(\kappa_m^+ a - \Delta_x^- a/2))$$

$$L = A_m a \operatorname{sinc}(\Delta_x^+ a/2) \exp(i(\kappa_m^+ a + \Delta_x^+ a/2))$$

$$M = C_m a \operatorname{sinc}(\Delta_x^- a/2) \exp(i(\kappa_m^+ a + \Delta_x^- a/2))$$

and

$$(3-16) \quad X_- = (U+V)\exp(i\kappa_m^+ x) + (W+Y)\exp(-i\kappa_m^+ x) ,$$

where

$$U = B_m a \operatorname{sinc}(\Delta_x^- a/2) \exp(-i(\kappa_m^+ a + \Delta_x^- a/2))$$

$$V = D_m a \operatorname{sinc}(\Delta_x^+ a/2) \exp(-i(\kappa_m^+ a + \Delta_x^+ a/2))$$

$$W = A_m a \operatorname{sinc}(\Delta_x^- a/2) \exp(i(\kappa_m^+ a - \Delta_x^- a/2))$$

$$Y = C_m a \operatorname{sinc}(\Delta_x^+ a/2) \exp(i(\kappa_m^+ a - \Delta_x^+ a/2))$$

and

$$(3-17) \quad Z = \exp(i\chi_m^+ z) \left[\frac{\exp(i\Delta_z z) - 1}{i\Delta_z} \right] .$$

Therefore, a typical term of Equation (3-11), after integrating with respect to x' and z' and fixing m , q , and s , is given by:

$$(3-18) \quad \phi_{\omega_{\pm}}(x, z) = -\frac{\omega_{\pm}}{4c_2} R Z (C_q^{\omega_1} C_s^{\omega_2} X_+ + C_q^{\omega_1^*} C_s^{\omega_2^*} X_-) ,$$

where * indicates a complex conjugate.

Chapter IV
NUMERICAL ANALYSIS

4.1 Determination of Axial Wavenumber

As discussed in Chapter II, eigenvalues of the layered waveguide system under consideration are determined by examining the poles of the Green's functions, $G_\chi(x|x',z')$, in wavenumber space. The real poles χ_m , obtained by setting $\Psi(\chi)=0$, are simply the real roots of Equation (2-26). As stated in Section 2.4, the axial wavenumber must lie in the range $k_1 \leq \chi_m \leq k_2$ for guided modes to propagate. Due to the periodicity of the tangent function, several different values of the form [see Equation (2-26)]:

$$(4-1) \quad G \cos(\kappa_{2m} a) = H \sin(\kappa_{2m} a) \quad ,$$

where

$$G = \rho_2 \rho_3 \kappa_{2m} \kappa_{1m} + \rho_1 \rho_2 \kappa_{2m} \kappa_{3m}$$

$$H = \rho_1 \rho_3 \kappa_{2m}^2 - \rho_2^2 \kappa_{1m} \kappa_{3m} \quad .$$

It is then obvious from Equation (4-1) that the first real root occurs for $\kappa_{2m} a$ in the range $0 \leq \kappa_{2m} a \leq \pi$, the second for

$\pi \leq \kappa_{2m} a \leq 2\pi$, and so on.²⁵ In general, then, the axial wavenumber for guided mode m represented by the positive real roots of Equation (4-1), χ_m , must lie in the range

$$(4-2) \quad \sqrt{k_2^2 - \left[\frac{m\pi}{a}\right]^2} \leq \chi_m \leq \sqrt{k_2^2 - \left[\frac{(m-1)\pi}{a}\right]^2}$$

Since $\chi_m > k_1$ for guided modes,²⁶ the lowest possible frequency that may propagate in mode m is given by:

$$(4-3) \quad f_{c_m} = \frac{(m-1)}{2a} \left[\frac{1}{c_2^2} - \frac{1}{c_1^2} \right]^{-\frac{1}{2}},$$

where f_{c_m} denotes cutoff frequency of the m^{th} mode.

The asymptotes described by the left-hand side of Equation (4-2) represent the limiting cases of "rigid" and "soft" (pressure release) boundaries on medium II since the eigenvalues of the systems are defined as

$$(4-4) \quad \kappa_{2m} = \frac{m\pi}{a} \quad m = 0, 1, 2, 3, \dots \quad 27$$

Symmetric and asymmetric modes for each condition are accounted for by m being even or odd (e.g., for rigid walls,

²⁵A listing of the FORTRAN program written to numerically determine the roots of Equation (4-1) is given in Appendix D.

²⁶See Section 2.4.

²⁷The $m=0$, or plane-wave, mode can occur only for rigid boundaries (see Appendix B).

m even implies symmetric modes; for soft walls, m even represents asymmetric modes). Figures 7 and 8 show the variation of the axial wavenumber, χ_m , with frequency for the first few modes of two, three-layer waveguides with semi-hard (Figure 7) and semi-soft (Figure 8) boundaries. The asymptotes given by Equation (4-2) are shown to represent perfectly rigid or soft walls. Since it was assumed that $c_3 > c_1 > c_2$, the cutoff frequency [Equation (4-3)] is independent of the speed of sound in medium III.

As shown in Figures 7 and 8, low frequencies tend to propagate at or near the phase velocity of the outer medium. With increasing frequency, the phase velocity asymptotically approaches the bulk speed of sound in medium II. This is the result of what is referred to in Section 2.8 as boundary-induced dispersion. The dispersivity exhibited by an acoustic, slow waveguide dramatically influences the behavior of nonlinearly generated spectral components. A discussion of these effects is presented following the next section.

4.2 Mode Shapes

As with any bounded system, each mode has its characteristic mode shape which is defined by the eigenfunctions of the system. The eigenmode expansions of

MEDIUM	PHASE VEL.*	DENSITY*	THICKNESS*	MODE	CUTOFF(kHz)
I	2000.0	2000.0	∞	1	0.00
II	500.0	2000.0	0.10	2	2.58
III	2000.0	2000.0	∞	3	5.16
				4	7.75

* SI UNITS

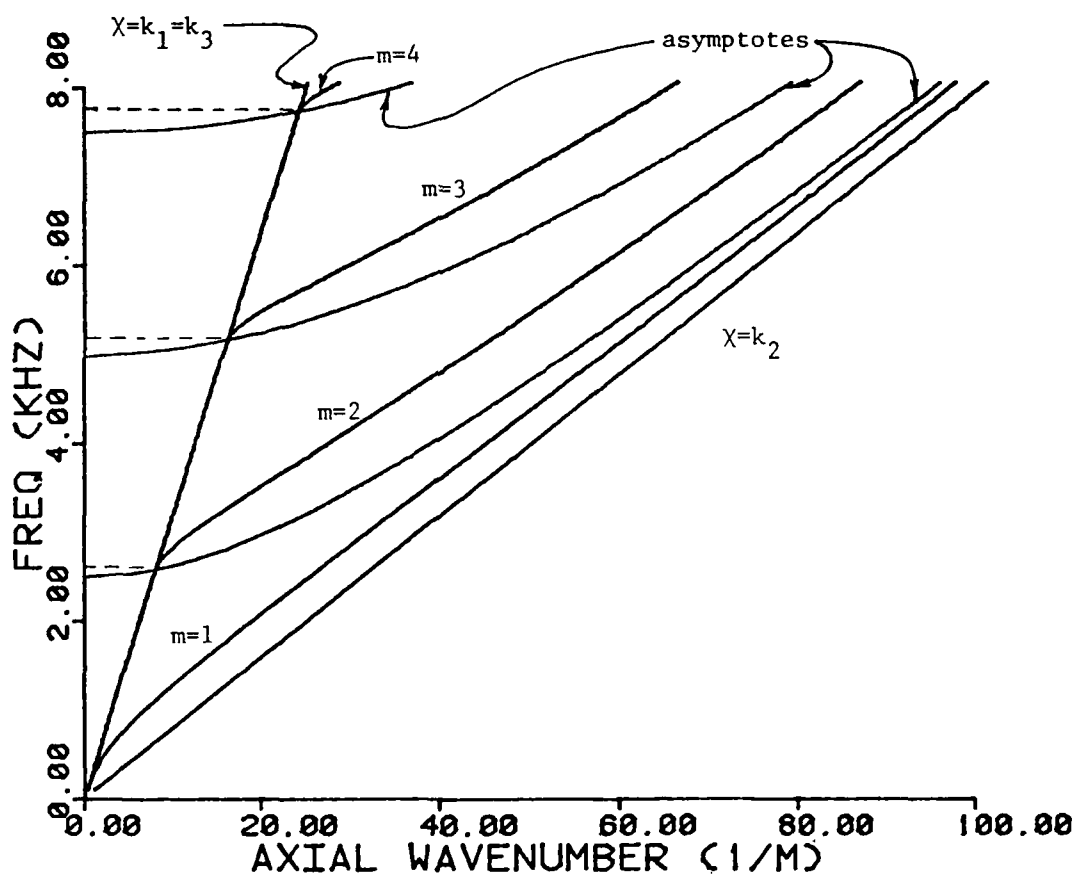


Figure 7. Dispersion relationship for first few guided modes in a 0.1 m.-thick waveguide bounded by semi-hard media. Dashed lines indicate cutoff frequencies for modes $m = 2, 3,$ and $4,$ and curves marked "asymptotes" are bounds for each mode (see Equation (4-2)).

MEDIUM	PHASE VEL.*	DENSITY*	THICKNESS*	MODE	CUTOFF(kHz)
I	2000.0	200.0	∞	1	0.00
II	500.0	2000.0	0.10	2	2.58
III	2000.0	200.0	∞	3	5.16
				4	7.75

* SI UNITS

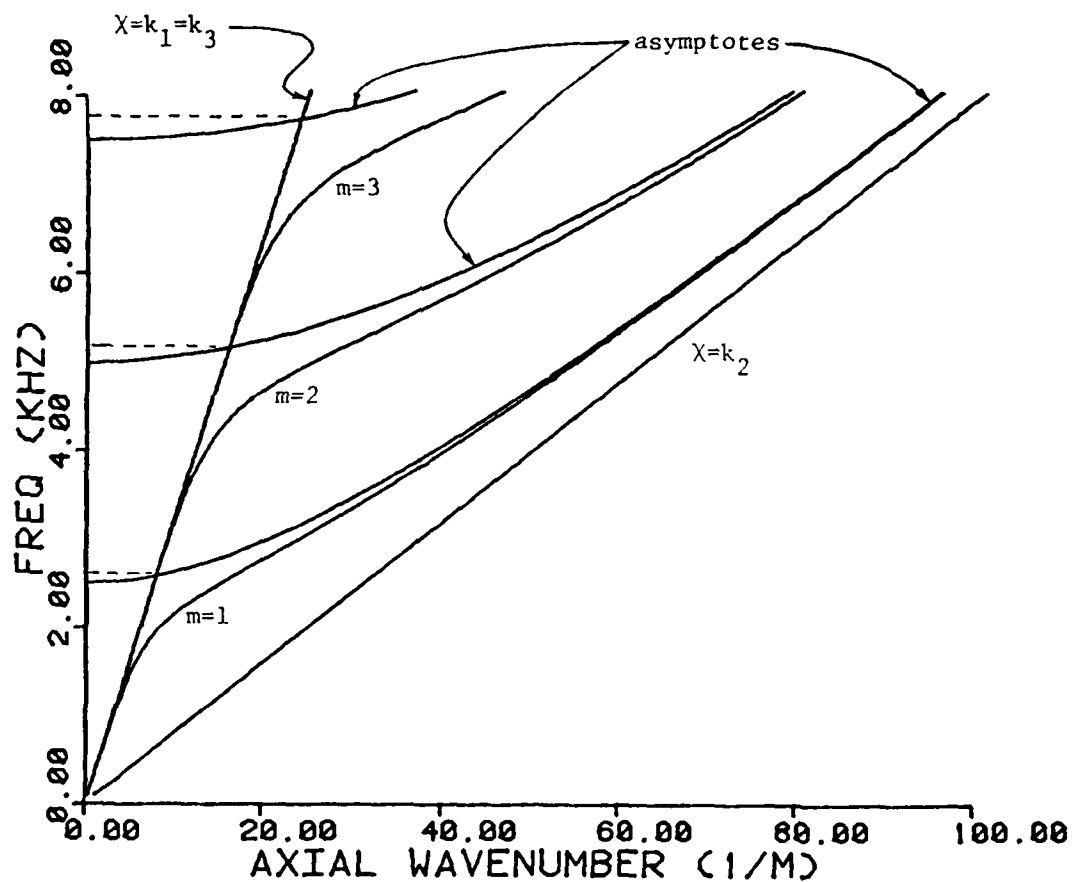


Figure 8. Dispersion relationship for first few guided modes in a 0.1 m.-thick waveguide bounded by semi-soft media. Dashed lines indicate cutoff frequencies for modes $m=2, 3$, and 4 , and curves marked "asymptotes" are bounds for each mode (see Equation (4-2)).

the velocity potential given in Chapter III, via Equations (3-4,5), may be re-expressed in terms of cosine and sine functions:

$$(4-5) \quad \phi_{\omega_1} = \sum_{q=-\infty}^{\infty} [A_q^{\omega_1} \cos(\kappa_{2q}^{\omega_1} x) + B_q^{\omega_1} \sin(\kappa_{2q}^{\omega_1} x)] \exp(i\chi_q^{\omega_1} z)$$

and

$$(4-6) \quad \phi_{\omega_2} = \sum_{s=-\infty}^{\infty} [C_s^{\omega_2} \cos(\kappa_{2s}^{\omega_2} x) + D_s^{\omega_2} \sin(\kappa_{2s}^{\omega_2} x)] \exp(i\chi_s^{\omega_2} z).$$

The velocity or pressure distribution of the source at the face of the waveguide (i.e., at $z=0$) determines the extent to which each mode is excited. If, for example, the velocity profile of a transducer, matched that of any single mode, then only that mode would propagate down the guide. The series expansion of Equation (4-5) would then be expressed as a single term representing the particular excited mode, while the coefficients $A_q^{\omega_1}$ and $B_q^{\omega_1}$ for all other modes would be identically zero. If, however, the end conditions are not perfectly matched, then several modes may be excited, all of whose cutoff frequencies are below the excitation frequency.²⁸

Since the transverse pressure distribution in medium II at a fixed range is proportional to the time derivative of

²⁸M. Redwood, Mechanical Waveguides (New York: Pergamon Press, 1960), pp. 77-84.

the velocity potential, then the variation with x , or the mode shape, is given by the transverse component of Equation (4-5) for a particular mode $q=m$:

$$(4-7) \quad F_m(x) = A_m \cos(\kappa_{2m} x) + B_m \sin(\kappa_{2m} x) ,$$

where coefficients A_m and B_m are determined by the source distribution. However, the ratio B_m/A_m may be found through application of boundary conditions to Equation (4-5) for guided modes:

$$(4-8) \quad \frac{B_m}{A_m} = \frac{\rho_2 \kappa_{3m}}{\rho_3 \kappa_{2m}} .$$

Thus, the function $F_m(x)$, normalized to A_m , becomes:

$$(4-9) \quad \frac{F_m(x)}{A_m} = \cos(\kappa_{2m} x) + \frac{\rho_2 \kappa_{3m}}{\rho_3 \kappa_{2m}} \sin(\kappa_{2m} x)$$

The coefficient A_m outside the brackets has no effect on the shape of individual modes and thus may be ignored.

The shape of the first three modes at various frequencies for a two-layered medium is depicted in Figures 9-11. These cases correspond to a large flat plate of silicone rubber immersed in water.

MEDIUM	PHASE VEL.*	DENSITY*	THICKNESS*	MODE	m=1
I	1500.0	1000.0	∞	CUTOFF(kHz)	0.00
II	1000.0	1000.0	0.10	FREQ. (kHz)	5.0
III	1500.0	1000.0	∞		10.0
					15.0

*SI UNITS

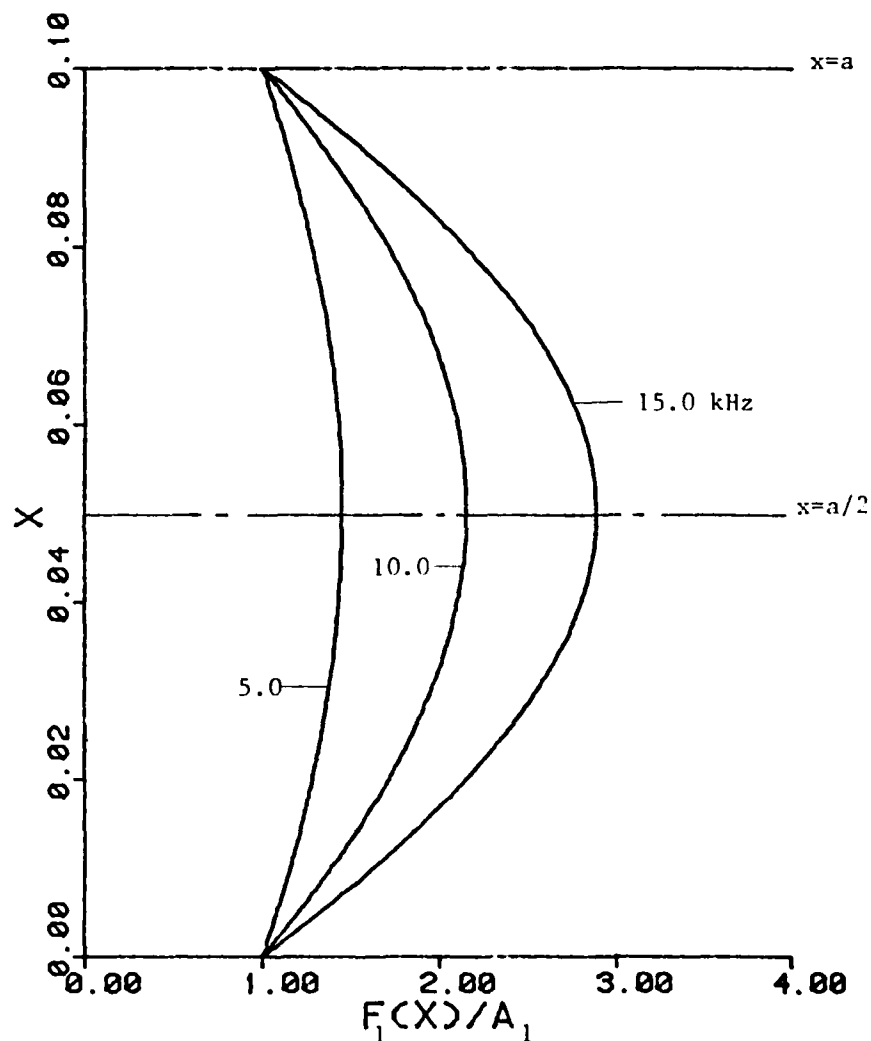


Figure 9. Transverse pressure distribution in medium II at fixed range for $m=1$ mode at 5, 10, and 15 kHz. Vertical axis represents vertical distance from medium III and horizontal axis is given by Equation (4-9). Physical parameters correspond to a 0.1m.-thick slab of silicone rubber immersed in water. SI units used.

MEDIUM	PHASE VEL.*	DENSITY*	THICKNESS*	MODE	m=2
I	1500.0	1000.0	∞	CUTOFF(kHz)	6.70
II	1000.0	1000.0	0.10	FREQ.(kHz)	10.0
III	1500.0	1000.0	∞		15.0
					20.0

* SI UNITS

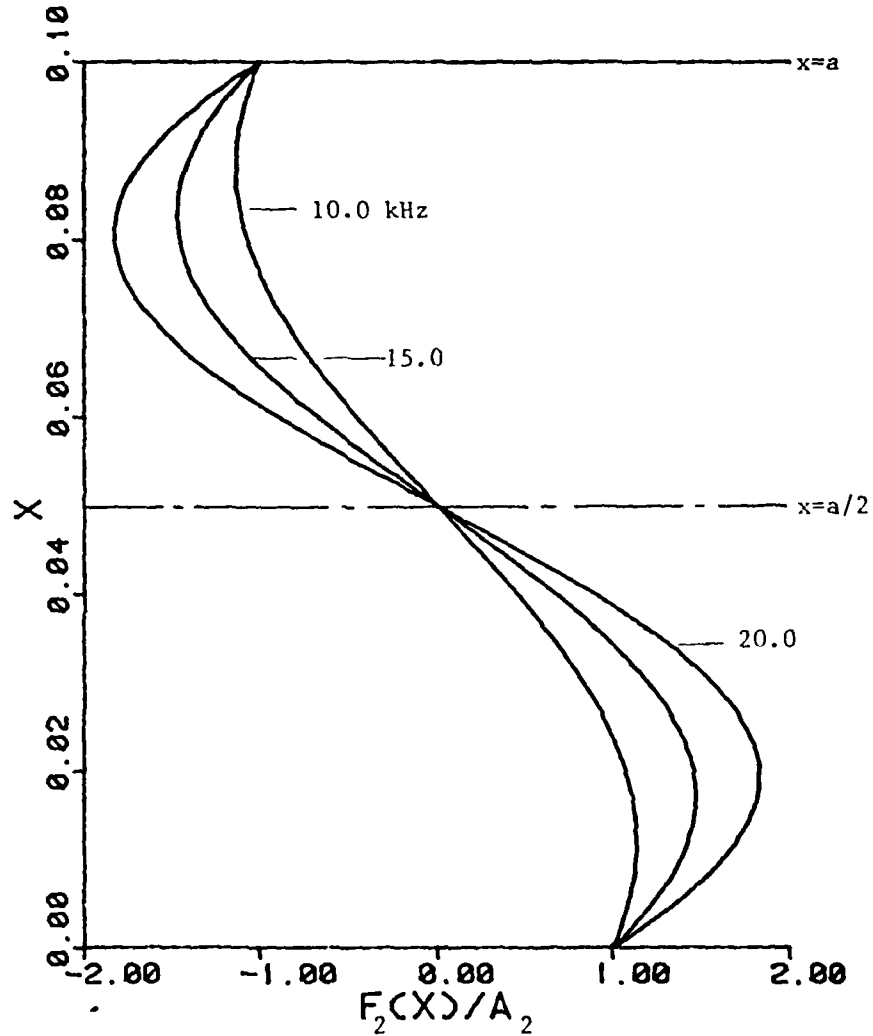


Figure 10. Transverse pressure distribution in medium II at fixed range for $m=2$ mode at 10, 15, and 20 kHz. Vertical axis represents vertical distance from medium III and horizontal axis is given by Equation (4-9). Physical parameters correspond to a 0.1m.-thick slab of silicone rubber immersed in water. SI units used.

MEDIUM	PHASE VEL.*	DENSITY*	THICKNESS*	MODE	m=3
I	1500.0	1000.0	∞	CUTOFF(kHz)	13.41
II	1000.0	1000.0	0.10	FREQ. (kHz)	15.0
III	1500.0	1000.0	∞		20.0
					25.0

* SI UNITS

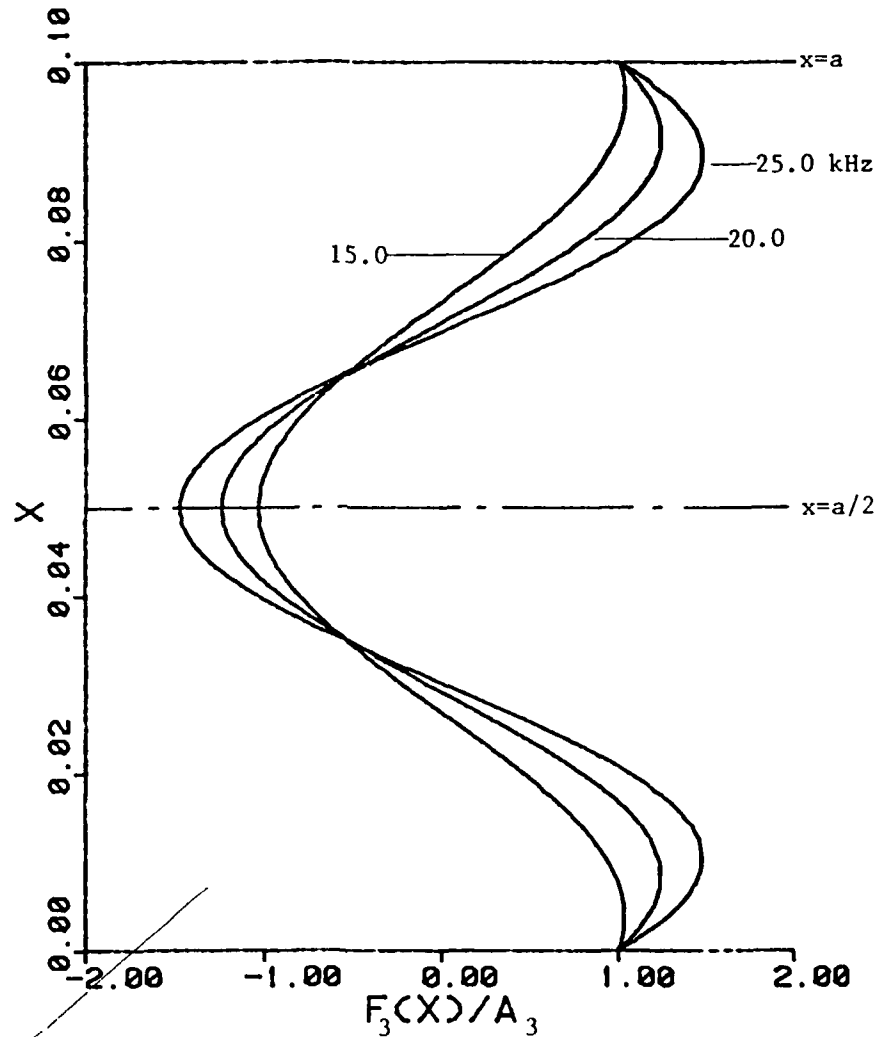


Figure 11. Transverse pressure distribution in medium II at fixed range for $m=3$ mode at 15, 20, and 25 kHz. Vertical axis represents vertical distance from medium III and horizontal axis is given by Equation (4-9). Physical parameters correspond to a 0.1m.-thick slab of silicone rubber immersed in water. SI units used.

Hence, the phase velocity and density correspond to previous experimental work.²⁹ It should be noted that the increase in amplitude at higher frequencies for each mode further demonstrates the effect of dispersion discussed above.

Finally, the variation of mode shape with changing boundary conditions for the lowest mode ($m=1$) is shown in Figure 12. The appearance of spreading seen for lower values of ρc (i.e., softer boundary conditions) at a given frequency is explained by Figures 7 and 8. The harder the boundaries, the less influence media I and III (which in all of the cases depicted are identical) have on the acoustic field in medium II.

4.3 Behavior of Nonlinearly Generated Components in Dispersive Media

The lowest spectral component produced by the nonlinear interaction of two primary waves of frequencies ω_1 and ω_2 is the difference frequency $\omega_- (= \omega_1 - \omega_2)$. The propagation constant of the volume source produced via interaction of the primary waves at this frequency is determined by a

²⁹J.D. Ryder, P.H. Rogers and J. Jarzynski, "Radiation of Difference-Frequency Sound Generated by Nonlinear Interaction in a Silicone Rubber Cylinder," Journal of the Acoustical Society of America, 59 (1976), 1077-1086; See also Figure 6.

vector combination of the primary wavenumbers. If this vector combination does not correspond to the natural propagation constant of the difference frequency in the medium, then asynchronous interaction will occur, resulting in the "spatial beating" effect depicted in Figure 13 for $\Delta_z > 0$. If, however, the primary waves which give rise to the difference-frequency component propagate at the same phase velocity as the latter, then Figure 13 shows that synchronous interaction or "spatial resonance" occurs (Figure 13, $\Delta_z = 0$). Under this condition, the amplitude of the nonlinearly generated component will grow monotonically with range until enough energy has been transferred from the primary waves to significantly reduce the strength of the volume source distribution (i.e., forcing function).

In general, the vector $\tilde{\Delta}$ is used to represent the wavenumber difference between the primary waves and nonlinearly generated frequency components. Thus, for the case of the sum- or difference-frequency components resulting from a bifrequency primary wave interaction,

$$(4-10) \quad \tilde{\Delta} = n\tilde{k}_1 \pm m\tilde{k}_2 - \tilde{k}_{nm} \quad .$$

In an unbounded, dispersionless medium, the resonance condition can be satisfied only if the wavefronts of the two waves are parallel and both propagate in the same direction. Under these conditions, the linear relationship between

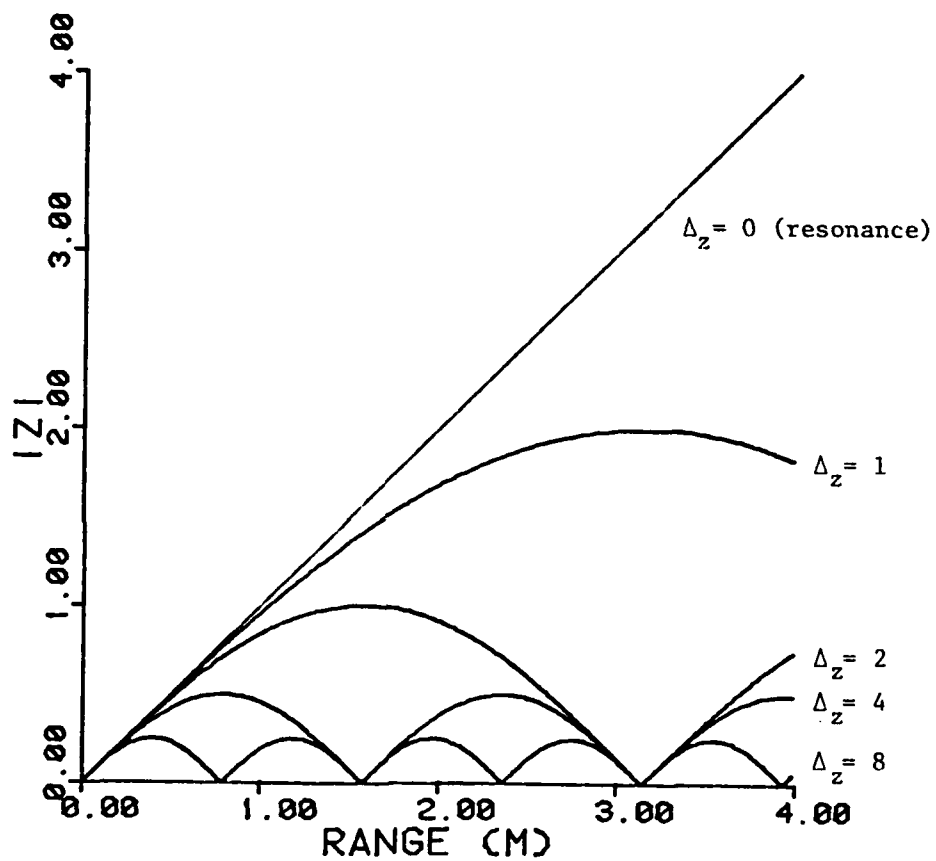


Figure 13. Magnitude of axial component of velocity potential, Z , in medium II as given by Equation (3-17) for several values of real Δ_z ($=1,2,4,8$), hence damping is neglected (i.e. $\alpha=0$).

wavenumber and frequency ($k=\omega/c$) necessitates synchronous interaction. However, in a dispersive medium such as a waveguide, resonant interaction is not so straightforward and will be treated in Section 4.4.

As previously stated, the analytical basis for Figure 13 may be found by examining the axial component of the velocity potential for the difference frequency in medium II, which was derived in Chapter III [i.e., Equation (3-17)]. Moreover, since acoustic waves in medium II may be characterized by their axial wavenumber for each mode, the vector $\tilde{\Delta}$ becomes a scalar quantity defined for the sum or difference frequency by

$$(4-11) \quad \Delta_z = \chi_q^{\omega_1} \pm \chi_s^{\omega_2} - \chi_m^{\omega_{\pm}} \quad ,$$

where the integer subscripts q , s , and m refer to the modes in which the primary frequencies (ω_1 and ω_2) and the sum or difference frequencies are respectively under consideration. The variation of the velocity potential with range is therefore described by the following equation from Chapter III:

$$(3-17) \quad Z = \exp(i\chi_m^{\omega_{\pm}} z) \left[\frac{\exp(i\Delta_z z) - 1}{i\Delta_z} \right] \quad .$$

where the magnitude of Z is plotted in Figure 13 for several real values of Δ_z . Notice that as Δ_z increases, the maximum allowable amplitude of the sum- or difference-frequency velocity potential decreases. In fact, the maximum allowable amplitudes $|Z|_{\max}$ occur at distances z_m from the source, where

$$(4-12) \quad |Z|_{\max} = |Z|_{z=z_m} = \frac{2}{\Delta_z}$$

$$(4-13) \quad z_m = \frac{m\pi}{\Delta_z} \quad m=1,3,5,\dots$$

Thus, in order to transfer as much energy as possible from the primaries into a nonlinearly generated frequency component, such as the sum or difference frequency, Δ_z must be minimized for that frequency.

It can be seen from Equation (4-12) that the maximum amplitude of the nonlinearly generated component can become extremely large for small Δ_z . In fact, for $\Delta_z=0$ (resonance), the amplitude grows linearly with range as shown by Figure 13. This apparently unrealistic situation may be resolved by considering the fact that the growth of a nonlinearly generated component is accompanied by the decay of the fundamental waves. Eventually, the decreased strength of the primary fields no longer permits a nonlinear interaction.

All real physical systems involve a certain amount of damping, which is accounted for by including an imaginary term in the axial wavenumbers.³⁰ In this instance, Equation (3-17) becomes:

$$(4-14) \quad Z = \exp(i\chi_m^{(\omega)} z) \exp(-\alpha_{\omega_{\pm}} z) \frac{1 - \exp(i\Delta_z z) \exp(-\alpha_T z)}{\alpha_T - i\Delta_z},$$

where α_T and $\alpha_{\omega_{\pm}}$ represent damping. The magnitude of Z given by Equation (4-14) versus range for fixed Δ_z , with absorption as the parameter, is illustrated in Figure 14.

4.4 Dispersion in Medium II

As established in the previous section, the maximum amount of energy transferred to any nonlinearly generated frequency component in a lossless, dispersive medium is determined by the difference in axial wavenumbers Δ_z .³¹ The term Δ_z as described by Equation (4-11) is a function of several independent variables. The χ_m versus ω relationships (e.g., Figures 7 and 8) which characterize the dispersivity of the waveguide are determined by the physical

³⁰Valid only for "weak" nonlinear interactions.

³¹See Equations (4-11) and (4-12).

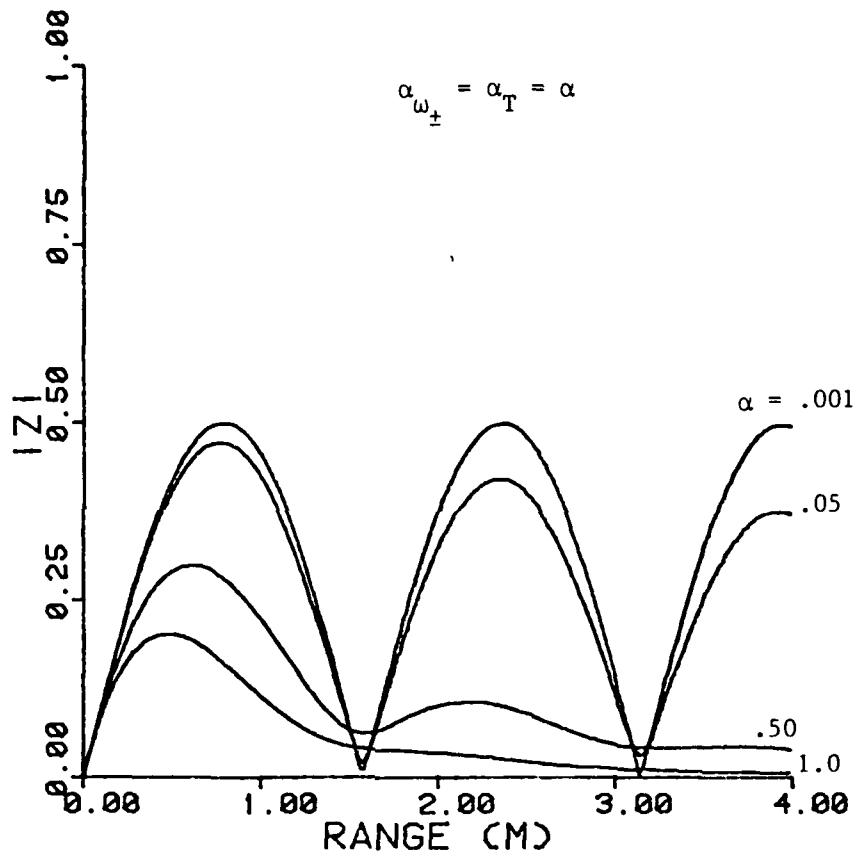


Figure 14. Magnitude of axial component of velocity potential, Z , in medium II as given by Equation (4-14) for $\Delta_z=4.0$ with increasing amounts of absorption (i.e., $\alpha=.001,.05,.5,1.0$). SI units used.

parameters of the media (i.e., density and bulk phase velocity of media I, II, and III, and thickness of medium II). Once this relationship is defined, Δ_z may be determined for the sum- or difference-frequency component of any given pair of primary waves, as long as it is known in which modes all four frequencies propagate.

The variation of Δ_z for the nonlinearly generated difference frequency ω_- for a fixed ratio ω_1/ω_- is shown in Figure 15. Again, the physical parameters are chosen to correspond with previous empirical data (i.e., silastic rubber in seawater).³² The primary waves as well as the difference frequency are assumed to propagate in the first mode.

³²See e.g., Ryder, Rogers, and Jarzynski, pp. 1077-1086.

MEDIUM	PHASE VEL.*	DENSITY*	THICKNESS*	PRIMARY MODE $q,s = 1$
I	1500.0	1000.0	∞	DIFF. FREQ. MODE $m = 1$
II	1000.0	1000.0	varies	FREQ. RATIO $f_1/f_- = 10$
III	1500.0	1000.0	∞	THICKNESS* = .05, .1, .2

* SI UNITS

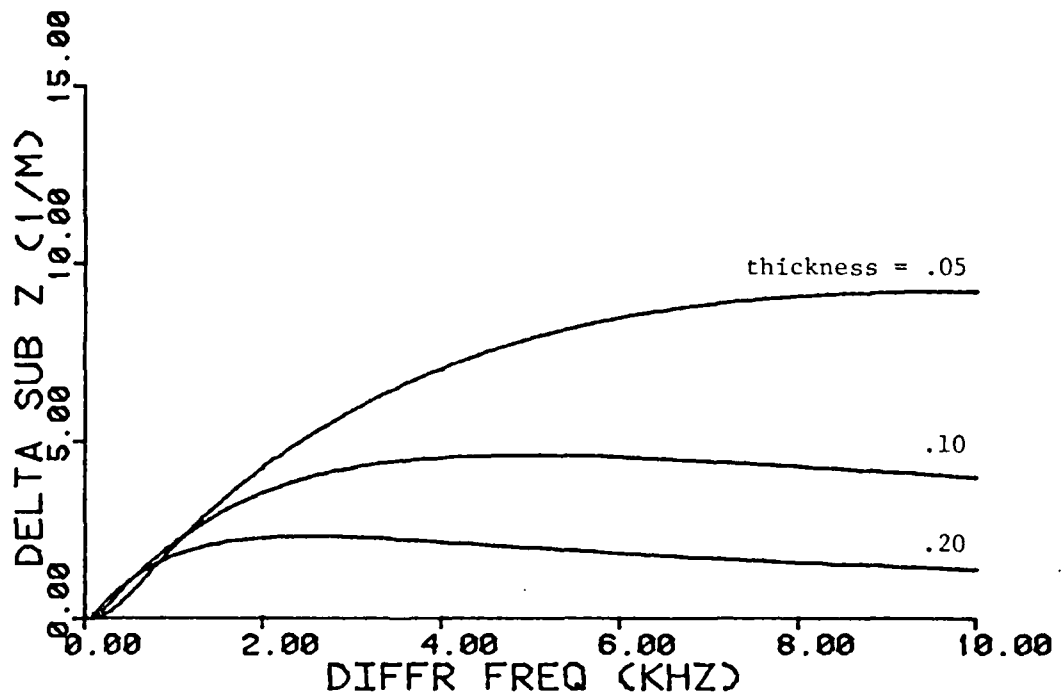


Figure 15. Variation of Δ_z with difference frequency (f_-) for fixed ratio of primary frequency (f_1) to f_- (i.e., $f_1/f_- = 10.0$). Phase velocities and densities correspond to silicone rubber immersed in water. It is assumed that the difference frequency as well as the primaries propagate in mode $m=1$. The three curves are for thicknesses of .05, .10, and .20 meters.

Chapter V

CONCLUSIONS

A theoretical investigation of weak, nonlinear acoustic wave interactions in a three-layered medium has been presented in this thesis. Under the conditions explained in Chapter I, an acoustic, slow waveguide has been analyzed both numerically and theoretically, and various characteristics of linear waveguide theory, as well as finite-amplitude phenomena, have been treated.

The dispersivity for guided mode propagation in an acoustic, slow waveguide is clearly defined by the characteristic equation derived in Chapter II. With the aid of the computer program listed in Appendix D, exact numerical data can be calculated given the physical parameters of the system. Once the dispersion relationship is established, the maximum allowable amplitude for any nonlinearly generated component may be calculated simply by determining the corresponding value of Δ_2 .

Expressions which may be used to determine the conversion efficiency of weak parametric interactions in simple, layered media (i.e., liquid-like media) have thus been developed. Moreover, a comparison of conversion-efficiency enhancement in a waveguide, relative to that in

an unbounded medium, can now be realized. However, in order to place an upper bound on conversion-efficiency enhancement via boundary-induced dispersion, a complete numerical analysis of strong wave interactions is required. Such an analysis, which would involve implementation via digital computer solution of many coupled partial differential equations, is outside the scope of this investigation. It is therefore recommended for future study.

APPENDIX A

Determination of $\left. \frac{\partial \Psi(\chi)}{\partial \chi} \right|_{\chi=\chi_m}$

From Equation (2-21):

$$(A-1) \quad \Psi(\chi) = (a+d)\sin(\kappa_2 a) + i(b+c)\cos(\kappa_2 a) \quad ,$$

where

$$a = \rho_2^3 \kappa_1 \kappa_3$$

$$b = \rho_1 \rho_2^2 \kappa_2 \kappa_3$$

$$c = \rho_2^2 \rho_3 \kappa_1 \kappa_2$$

$$d = \rho_1 \rho_2 \rho_3 \kappa_2^2$$

Then, the derivative is given by:

$$(A-2) \quad \Psi'(\chi_m) = \left. \frac{\partial \Psi}{\partial \chi} \right|_{\chi=\chi_m}$$

$$= \left. \frac{\partial \Psi}{\partial \kappa_1} \frac{\partial \kappa_1}{\partial \chi} + \frac{\partial \Psi}{\partial \kappa_2} \frac{\partial \kappa_2}{\partial \chi} + \frac{\partial \Psi}{\partial \kappa_3} \frac{\partial \kappa_3}{\partial \chi} \right|_{\chi=\chi_m}$$

Also ,

$$(A-3) \quad \frac{\partial \kappa_i}{\partial \chi} = - \frac{\chi}{\kappa_i} \quad i = 1, 2, 3$$

and

$$(A-4) \quad \frac{\partial \Psi}{\partial \kappa_1} = \rho_2^3 \kappa_3 \sin(\kappa_2 a) + i \rho_2^2 \rho_3 \kappa_2 \cos(\kappa_2 a) \quad ,$$

$$(A-5) \quad \frac{\partial \Psi}{\partial \kappa_2} = (\rho_1 \rho_2 \rho_3 \kappa_2^2 a + \rho_2^3 \kappa_1 \kappa_3 a + i \rho_2^2 \rho_3 \kappa_1 + i \rho_1 \rho_2^2 \kappa_3) \cos(\kappa_2 a) + \\ (2\rho_1 \rho_2 \rho_3 \kappa_2 - i \rho_2^2 \rho_3 \kappa_1 \kappa_2 a - i \rho_1 \rho_2^2 \kappa_2 \kappa_3 a) \sin(\kappa_2 a) ,$$

$$(A-6) \quad \frac{\partial \Psi}{\partial \kappa_3} = \rho_2^3 \kappa_1 \sin(\kappa_2 a) + i \rho_1 \rho_2^2 \kappa_2 \cos(\kappa_2 a) .$$

Therefore ,

$$(A-7) \quad \Psi'(\chi_m) = \chi_m \left[(\rho_2^3 \frac{\kappa_{3m}^2 + \kappa_{1m}^2}{\kappa_{1m} \kappa_{3m}} + 2\rho_1 \rho_2 \rho_3 + \rho_2^2 \rho_3 \kappa_{1m} a + \right. \\ \left. \rho_1 \rho_2^2 \kappa_{3m} a) \sin(\kappa_{2m} a) + (\rho_1 \rho_2 \rho_3 \kappa_{2m} a + \right. \\ \left. \rho_2^2 \rho_3 \frac{\kappa_{2m}}{\kappa_{1m}} - \frac{\rho_2^2 \rho_3 \kappa_{1m} + \rho_2^3 \kappa_{1m} \kappa_{3m} a + \rho_1 \rho_2^2 \kappa_{3m}}{\kappa_{2m}} + \right. \\ \left. \rho_1 \rho_2^2 \frac{\kappa_{2m}}{\kappa_{3m}}) \cos(\kappa_{2m} a) \right] ,$$

where

$$\kappa_1 = i \kappa_{1m}$$

$$\kappa_2 = \kappa_{2m}$$

$$\kappa_3 = i \kappa_{3m} .$$

Appendix B

PLANE-WAVE MODE

As discussed in Chapter II, the Green's functions for the waveguide are expressed as a summation of the residues of the transformed Green's functions, G_χ , at the real poles χ_m of G_χ . The real roots of Equation (2-26), restated here, represent these poles:

$$(B-1) \quad \tan(\kappa_{2m} a) = \frac{\kappa_{1m} \kappa_{2m} \rho_2 \rho_3 + \kappa_{2m} \kappa_{3m} \rho_1 \rho_2}{\kappa_{2m} \rho_1 \rho_3 - \kappa_{1m} \kappa_{3m} \rho_2}$$

One root in particular of this equation, $\chi_m = k_2$ (or $\kappa_{2m} = 0$), is not consistent with physical or mathematical assumptions. It is the purpose of this section to examine the behavior of G_χ at the root $\chi_m = k_2$ and to determine its physical significance.

Assume, as in Equation (2-27), that G_χ is expressible in the form

$$(B-2) \quad G_\chi(x|x', z') = \exp(i\chi(z-z')) \frac{F(\chi)}{\Psi(\chi)},$$

where $\Psi(\chi)$ is given in Equation (2-21), and $F(\chi)$, which changes with each region, may be deduced from Equations (2-15)-(2-18). For region IIA (i.e., $a \geq x \geq x'$);

$$(B-3) \quad F(\chi) = \frac{A \exp(-i(\theta-\phi)) + B \exp(i(\theta+\phi)) + C \exp(-i(\theta+\phi)) + D \exp(i(\theta-\phi))}{4\kappa_2},$$

where

$$\theta = \kappa_2(x-a)$$

$$\phi = \kappa_2 x'$$

and coefficients A, B, C, and D are given by Equation (2-20). Then, since

$$(B-4) \quad \lim_{\kappa_2 \rightarrow 0} \left[\frac{F(\chi)}{\Psi(\chi)} \right]$$

is indeterminate, L'Hopital's Rule may be applied with the following results:

$$(B-5) \quad \lim_{\chi \rightarrow k_2} G_\chi = \lim_{\chi \rightarrow k_2} \left[\frac{\left. \frac{\partial F(\chi)}{\partial \chi} \right|_{\chi = \chi_m = k_2}}{\left. \frac{\partial \Psi(\chi)}{\partial \chi} \right|_{\chi = \chi_m = k_2}} \right]$$

$$= \frac{-\kappa_{1m}(x-a) + \kappa_{3m}x' - \kappa_{1m}\kappa_{3m}(x'(x-a)) + 1}{\kappa_{1m} + \kappa_{3m} + \kappa_{1m}\kappa_{3m}a}$$

Thus, for guided modes, κ_{1m} and κ_{3m} are both positive real values; therefore, the transformed Green's function G_χ in region IIA remains finite at $\chi_m = k_2$. Hence, $k_2 = \chi$ is not a singularity of G_χ even though it is a root of Equation (2-26). A similar process verifies that for all regions (i.e., I, IIA, IIB, and III),

$$(B-6) \quad \lim_{\kappa_2 \rightarrow 0} \left[G_\chi(x|x') \right]$$

remains finite. Physically, this means that an incoming wave propagating purely in the axial direction of the waveguide (i.e., $\chi_m = k_2$ implies a planar wavefront) will not propagate as a trapped wave, but will decay as energy is radiated to the outer media. If, however, medium II had rigid boundaries, then the plane-wave mode would propagate as a guided mode.

Appendix C

GREEN'S FUNCTIONS FOR MEDIA I AND III

Expressions derived in Chapter II for G_m^+ represent Green's functions for medium II only. That is, it was assumed that the point source was in the waveguide (recall that $0 \leq x' \leq a$). If, however, sources occurred outside the guide, or energy originally radiated from the guide penetrated back into medium II via some coupling mechanism (e.g., corrugated surface structure), then Green's functions for media I and III would be required in order to evaluate these effects.

As discussed in Chapter II, the transformed Green's functions G_χ , for the waveguide, were derived for each region and are given by Equations (2-15)-(2-18). In order to distinguish these from the following expressions which are obtained by assuming the point source is in medium I or III, a superscript will be used to denote medium number (i.e., G_χ^I and G_χ^{III} correspond to the point source in media I and III, respectively).

The matrix equations whose solutions determine the transformed Green's functions for media I and III are given

$$\begin{bmatrix} 0 \\ \exp(i\kappa_1 x') \\ 0 \\ 0 \\ 0 \\ -i\kappa_1 \exp(i\kappa_1 x') \end{bmatrix}
 \begin{bmatrix} \rho_1 \exp(i\kappa_1 a) \\ -\exp(i\kappa_1 x') \\ 0 \\ \kappa_1 \exp(i\kappa_1 a) \\ 0 \\ i\kappa_1 \exp(i\kappa_1 x') \end{bmatrix}
 \begin{bmatrix} \rho_1 \exp(-i\kappa_1 a) \\ -\exp(-i\kappa_1 x') \\ 0 \\ -\kappa_1 \exp(-i\kappa_1 a) \\ 0 \\ -i\kappa_1 \exp(-i\kappa_1 x') \end{bmatrix}
 \begin{bmatrix} -\rho_2 \exp(i\kappa_2 a) \\ 0 \\ \rho_2 \\ -\kappa_2 \exp(i\kappa_2 a) \\ \kappa_2 \\ 0 \end{bmatrix}
 \begin{bmatrix} -\rho_2 \exp(-i\kappa_2 a) \\ 0 \\ \rho_3 \\ \kappa_2 \exp(-i\kappa_2 a) \\ \kappa_2 \\ 0 \end{bmatrix}
 \begin{bmatrix} 0 \\ 0 \\ \rho_3 \\ 0 \\ \kappa_3 \\ 0 \end{bmatrix}
 \times
 \begin{bmatrix} A_1 \\ B_1 \\ B_2 \\ C_1 \\ C_2 \\ D_2 \end{bmatrix}
 =
 \begin{bmatrix} 0 \\ 0 \\ 0 \\ 0 \\ 0 \\ \exp(-iXz') \end{bmatrix}$$

Equation (C-1)

$$\begin{bmatrix} \rho_1 \exp(i\kappa_1 a) \\ 0 \\ 0 \\ \kappa_1 \exp(i\kappa_1 a) \\ 0 \\ 0 \end{bmatrix}
 \begin{bmatrix} -\rho_2 \exp(i\kappa_2 a) \\ 0 \\ \rho_2 \\ -\kappa_2 \exp(i\kappa_2 a) \\ \kappa_2 \\ 0 \end{bmatrix}
 \begin{bmatrix} -\rho_2 \exp(-i\kappa_2 a) \\ \exp(i\kappa_3 x') \\ -\rho_3 \\ \kappa_2 \exp(-i\kappa_2 a) \\ -\kappa_3 \\ 0 \end{bmatrix}
 \begin{bmatrix} 0 \\ \exp(i\kappa_3 x') \\ -\rho_3 \\ 0 \\ -i\kappa_3 \exp(i\kappa_3 x') \\ i\kappa_3 \exp(-i\kappa_3 x') \end{bmatrix}
 \begin{bmatrix} -\exp(-i\kappa_3 x') \\ 0 \\ 0 \\ 0 \\ \kappa_3 \\ -i\kappa_3 \exp(-i\kappa_3 x') \end{bmatrix}
 \begin{bmatrix} 0 \\ 0 \\ 0 \\ 0 \\ 0 \\ \exp(-iXz') \end{bmatrix}$$

Equation (C-2)

by Equations (C-1) and (C-2), respectively.

Following are expressions for the transformed Green's functions for medium I (i.e., $x' \geq a$):

Region IA, $x \geq x'$:

$$(C-3) \quad G_{\chi}^I = \exp(-i\chi z') \exp(i\kappa_1 x) \left[\frac{\exp(i\kappa_2 a) [C \exp(i\kappa_1 (x'-a)) + D \exp(-i\kappa_1 (x'-a))] + \exp(-i\kappa_2 a) [E \exp(i\kappa_1 (x'-a)) + F \exp(-i\kappa_1 (x'-a))]}{\Psi(\chi)} \right]$$

Region IB, $x' \geq x \geq a$:

$$(C-4) \quad G_{\chi}^I = \exp(-i\chi z') \exp(i\kappa_1 x') \left[\frac{\exp(i\kappa_2 a) [C \exp(i\kappa_1 (x-a)) + D \exp(-i\kappa_1 (x-a))] + \exp(-i\kappa_2 a) [E \exp(i\kappa_1 (x-a)) + F \exp(-i\kappa_1 (x-a))]}{\Psi(\chi)} \right]$$

Region II, $a \geq x \geq 0$:

$$(C-5) \quad G_{\chi}^I = 4 \exp(-i\chi z') \exp(i\kappa_1 x') \frac{\rho_1 \rho_3 \kappa_1 \kappa_2 \cos(\kappa_2 x) - i \rho_1 \rho_2 \kappa_1 \kappa_3 \sin(\kappa_2 x)}{\Psi(\chi)}$$

Region III, $x \leq 0$:

$$(C-6) \quad G_{\chi}^I = \frac{\rho_1 \rho_2 \kappa_1 \kappa_2^4 \exp(-i\chi z') \exp(-i\kappa_3 x) \exp(i\kappa_1 x')}{\Psi(\chi)}$$

The transformed Green's functions for medium III (i.e., $x' \leq 0$) are:

Region I, $x \geq a$:

$$(C-7) \quad G_X^{III} = \frac{4\rho_2\rho_3\kappa_2\kappa_3 \exp(-i\chi z') \exp(-i\kappa_3 x') \exp(i\kappa_1 x)}{\Psi(\chi)}$$

Region II, $a \geq x \geq 0$:

$$(C-8) \quad G_X^{III} = 4 \exp(-i\chi z') \exp(i\kappa_1 a) \exp(-i\kappa_3 x') \left[\frac{\rho_2 \rho_3 \kappa_1 \kappa_3 \cos(\kappa_2(x-a)) + i \rho_1 \rho_3 \kappa_2 \kappa_3 \sin(\kappa_2(x-a))}{\Psi(\chi)} \right]$$

Region IIIA, $x' \leq x \leq 0$:

$$(C-9) \quad G_X^{III} = \exp(-i\chi z') \exp(i\kappa_1 a) \exp(-i\kappa_3 x') \left[\frac{\exp(i\kappa_3 x) [D \exp(i\kappa_2 a) + F \exp(-i\kappa_2 a)] + \exp(-i\kappa_3 x) [G \exp(i\kappa_2 a) + H \exp(-i\kappa_2 a)]}{\Psi(\chi)} \right]$$

Region IIIB, $x \leq x'$:

$$(C-10) \quad G_X^{III} = \exp(-i\chi z') \exp(i\kappa_1 a) \exp(-i\kappa_3 x) \left[\frac{\exp(i\kappa_2 a) [D \exp(i\kappa_3 x') + F \exp(-i\kappa_3 x')] + \exp(-i\kappa_2 a) [G \exp(i\kappa_3 x') + H \exp(-i\kappa_3 x')]}{\Psi(\chi)} \right]$$

The Green's functions are then obtained via an inverse transformation involving complex integration techniques (i.e., residue theory) as outlined in Chapter II. Following are the results for media I and III.

Green's functions for the m^{th} forward-guided mode for medium I are:

Region IA, $x > x'$:

$$(C-11) \quad G_m^I = 2\pi i \exp(i\chi_m(z-z')) \exp(-\kappa_{1m}x) \left[\frac{\exp(i\kappa_{2m}a) [C_m \exp(-\kappa_{1m}(x'-a)) + D_m \exp(\kappa_{1m}(x'-a))] + \exp(-i\kappa_{2m}a) [E_m \exp(-\kappa_{1m}(x'-a)) + F_m \exp(\kappa_{1m}(x'-a))]}{\Psi'(\chi_m)} \right]$$

Region IB, $x' > x > a$:

$$(C-12) \quad G_m^I = 2\pi i \exp(i\chi_m(z-z')) \exp(-\kappa_{1m}x') \left[\frac{\exp(\kappa_{1m}(a-x)) [C_m \exp(i\kappa_{2m}a) + E_m \exp(-i\kappa_{2m}a)] + \exp(-\kappa_{1m}(a-x)) [D_m \exp(i\kappa_{2m}a) + F_m \exp(-i\kappa_{2m}a)]}{\Psi'(\chi_m)} \right]$$

Region II, $a \geq x \geq 0$:

$$(C-13) \quad G_m^I = -8\pi \exp(i\chi_m(z-z')) \exp(-\kappa_{1m}x') \left[\frac{\rho_1 \rho_3 \kappa_{1m} \kappa_{2m} \cos(\kappa_{2m}x) + \rho_1 \rho_2 \kappa_{1m} \kappa_{3m} \sin(\kappa_{2m}x)}{\Psi'(\chi_m)} \right]$$

Region III, $x \leq 0$:

$$(C-14) \quad G_m^I = \frac{-8\pi \rho_1 \rho_2 \kappa_{1m} \kappa_{2m} \exp(i\chi_m(z-z')) \exp(\kappa_{3m}x) \exp(-\kappa_{1m}x')}{\Psi'(\chi_m)}$$

And the Green's functions for medium III are:

Region I, $x \geq a$:

$$(C-15) \quad G_m^{III} = \frac{-8\pi \rho_2 \rho_3 \kappa_{2m} \kappa_{3m} \exp(i\chi_m(z-z')) \exp(\kappa_{3m}x') \exp(-\kappa_{1m}x)}{\Psi'(\chi_m)}$$

Region II, $a \geq x \geq 0$:

$$(C-16) \quad G_m^{III} = -8\pi i \exp(i\chi_m(z-z')) \exp(-\kappa_{1m}a) \exp(\kappa_{3m}x') \times \frac{\rho_2 \rho_3 \kappa_{1m} \kappa_{3m} \cos(\kappa_{2m}(x-a)) + \rho_1 \rho_3 \kappa_{2m} \kappa_{3m} \sin(\kappa_{2m}(x-a))}{\Psi'(\chi_m)}$$

Region IIIA, $x' \leq x \leq 0$:

$$(C-17) \quad G_m^{III} = 2\pi i \exp(iX_m(z-z')) \exp(-\kappa_{1m}a) \exp(\kappa_{3m}x') \times$$

$$\left[\frac{\exp(-\kappa_{3m}x) [D_m \exp(i\kappa_{2m}a) + F_m \exp(-i\kappa_{2m}a)]}{\Psi'(X_m)} + \right.$$

$$\left. \frac{\exp(\kappa_{3m}x) [G_m \exp(i\kappa_{2m}a) + H_m \exp(-i\kappa_{2m}a)]}{\Psi'(X_m)} \right]$$

Region IIIB, $x \leq x'$:

$$(C-18) \quad G_m^{III} = 2\pi i \exp(iX_m(z-z')) \exp(-\kappa_{1m}a) \exp(\kappa_{3m}x) \times$$

$$\left[\frac{\exp(i\kappa_{2m}a) [D_m \exp(-\kappa_{3m}x') + G_m \exp(\kappa_{3m}x')]}{\Psi'(X_m)} + \right.$$

$$\left. \frac{\exp(-i\kappa_{2m}a) [F_m \exp(-\kappa_{3m}x') + H_m \exp(\kappa_{3m}x')]}{\Psi'(X_m)} \right]$$

where the following substitutions have been made in Equations (C-3) - (C-10);

$$(C-19) \quad \Psi(\chi) = 2i \exp(i\kappa_1 a) [A \exp(i\kappa_2 a) + B \exp(-i\kappa_2 a)]$$

$$(C-20) \quad a = \rho_2 \rho_3 \kappa_1 \kappa_2$$

$$b = \rho_1 \rho_3 \kappa_2^2$$

$$c = \rho_2^2 \kappa_1 \kappa_3$$

$$d = \rho_1 \rho_2 \kappa_2 \kappa_3$$

AD-A085 185

PENNSYLVANIA STATE UNIV UNIVERSITY PARK APPLIED RESE--ETC F/6 20/1
NONLINEAR ACOUSTIC WAVE INTERACTIONS IN LAYERED MEDIA.(U)
MAR 80 D M YEAGER N00024-79-C-6043

UNCLASSIFIED

TM-80-32

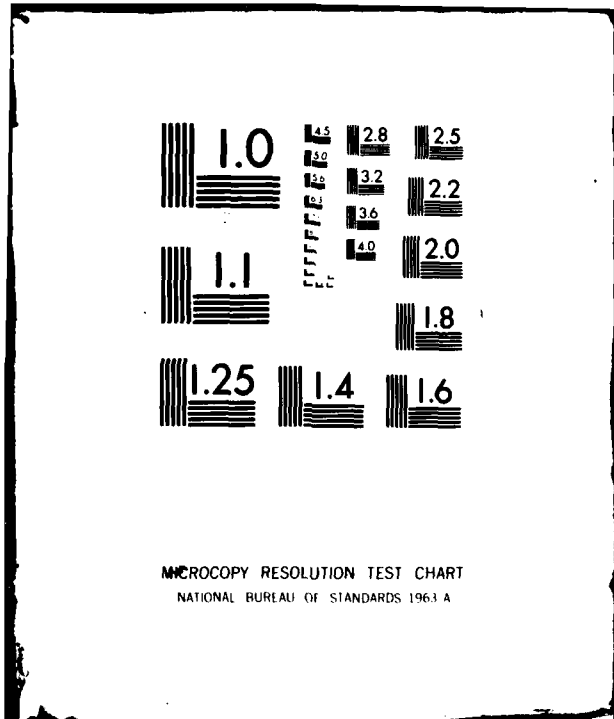
NL

2 v 2

2 of 2



END
DATE
FILMED
6 80
DTIC



MICROCOPY RESOLUTION TEST CHART
NATIONAL BUREAU OF STANDARDS 1963 A

$$\begin{aligned}
 \text{(C-21)} \quad A &= -a+b+c-d & E &= a-b+c-d \\
 B &= -a-b-c-d & F &= a+b+c+d \\
 C &= a+b-c-d & G &= -a+b-c+d \\
 D &= a-b-c+d & H &= -a-b+c+d .
 \end{aligned}$$

Equations (C-11) through (C-18) represent, as in Chapter II, the m^{th} guided mode in an eigenmode expansion of the Green's functions. The poles of G_χ are found by setting Equation (C-19), $\Psi(\chi)=0$. Then, for guided modes

$$\begin{aligned}
 \text{(C-22)} \quad \kappa_1 &= i\kappa_{1m} \\
 \kappa_2 &= \kappa_{2m} \\
 \kappa_3 &= i\kappa_{3m}
 \end{aligned}$$

and the terms given by Equation (C-20) become:

$$\begin{aligned}
 \text{(C-23)} \quad a_m &= i\rho_2\rho_3\kappa_{1m}\kappa_{2m} \\
 b_m &= \rho_1\rho_3\kappa_{2m}^2 \\
 c_m &= -\rho_2^2\kappa_{1m}\kappa_{3m} \\
 d_m &= i\rho_1\rho_2\kappa_{2m}\kappa_{3m} .
 \end{aligned}$$

The coefficients A_m, B_m, \dots, H_m are the same functions as given in Equation (C-21) except for the use of the subscripted variables defined in Equation (C-23) in place of the a, b, c, d found in Equation (C-20).

Notice that the determinants of the matrices of Equations (C-1) and (C-2) are equal [Equation (C-19)], but

differ from the determinant found in Chapter II [Equation (2-21)]. The derivative of Equation (C-19) evaluated at the poles $x = x_m$,

$$(C-24) \quad \psi'(x_m) = \left. \frac{\partial \psi(x)}{\partial x} \right|_{x=x_m},$$

therefore should not be confused with the expression derived in Appendix A, Equation (A-7), which was restated in Chapter II. This expression [Equation (2-38)] is derived by assuming the point source lies in medium II.

Appendix D

NUMERICAL EVALUATION OF EIGENVALUES:
COMPUTER PROGRAM LISTING

The FORTRAN program named AXIAL (Figure 16) was written by the author for the purpose of numerically investigating various characteristics of an acoustic, slow waveguide. The eigenvalues of the guided modes in medium II are obtained by evaluating the real roots of the characteristic equation

$$(D-1) \quad \tan(\kappa_{2m} a) = \frac{\rho_2 \rho_3 \kappa_{1m} \kappa_{2m} + \rho_1 \rho_2 \kappa_{2m} \kappa_{3m}}{\rho_1 \rho_3 \kappa_{2m}^2 - \rho_2 \kappa_{1m} \kappa_{3m}} = \frac{G}{H}$$

In order to avoid numerical problems at the discontinuities of the tangent function, a similar form of Equation (D-1) was used in the program:³³

$$(D-2) \quad F(x) = G \cos(\kappa_{2m} a) - H \sin(\kappa_{2m} a)$$

AXIAL utilizes an IMSL subroutine (ZBRENT) to locate the real roots of an external function $F(x)$. These real roots are stored in a multidimensional array TRAP(m,n) where

³³See also Equation (4-1).

"m" denotes mode and "n" frequency number. Since ZBRENT was designed to locate the root x' of a function between any two endpoints a and b such that the product of $F(a)$ and $F(b)$ is less than zero, care must be taken to insure that exactly one root exists in that interval before executing ZBRENT. It follows from the discussion in Section 4.1 that the m^{th} real root χ_m lies between the asymptotes described in equation (4-2). Hence, the interval containing one and only one root of $F(x)$ is well defined.

Once the roots have been located and stored, the array TRAP is plotted via the CCS graphics system supported by The Pennsylvania State University Computation Center.³⁴ Examples of the graphics output may be seen in Figures 6, 7, and 8.

³⁴ CCS is an abbreviation for California Computer Products, Inc. (CalComp) who originally developed the software.

```

C-----
C AUTHOR:
C   DAVID M. YEAGER
C   ACOUSTICS DEPARTMENT
C   PENNSYLVANIA STATE UNIVERSITY
C
C DATE WRITTEN:
C   AUGUST 22, 1979
C
C PROGRAM NAME:
C   AXIAL
C
C PURPOSE:
C   THE PURPOSE OF THIS PROGRAM IS TO COMPUTE THE POSITIVE, REAL ROOTS
C   X OF AN EXTERNAL FUNCTION F(X) WHERE 'F' IN THIS CASE IS THE
C   CHARACTERISTIC EQUATION FOR A TWO-DIMENSIONAL FLAT-PLATE 'SLOW'
C   WAVEGUIDE. HENCE THE PHASE VELOCITY IN MEDIUM TWO IS LESS THAN
C   IN MEDIA 1 OR 3. IN FACT IT IS ASSUMED THAT  $C_3 > C_1 > C_2$ .
C   THESE ROOTS REPRESENT THE EIGENVALUES OF THE GUIDE AND ARE
C   GROUPED ACCORDING TO MODES BEFORE BEING PLOTTED. THE VERTICAL
C   AXIS IS FREQUENCY AND WAVENUMBER IN THE AXIAL DIRECTION IS
C   DISPLAYED ON THE HORIZONTAL AXIS.
C-----
C   REAL*8 EPS,A,B,F
C   REAL MAXFR
C   CHARACTER*8 DA
C   DIMENSION GAM1(202),GAM2(202),GAM3(202),FRQ(202),TRAP(10,202),
C   CFC(30),ALPH1(202),ALPH2(202),ALPH3(202),DELTA(202),C(3),R(3)
C   COMMON/AREA1/GAM1I,GAM2I,GAM3I,RO1,RO2,RO3,I,THICK
C
C   SEE LISTING OF ZBRENT FOR EXPLANATION OF 'EPS,NSIG,MAXFN'
C   'C1,C2,C3' REPRESENT BULK PHASE VELOCITIES FOR MEDIA 1,2,3
C   RESPECTIVELY. 'THICK' IS TOTAL THICKNESS OF MEDIUM 2 SINCE THE
C   BOUNDARIES ARE AT X=0, AND X=A. 'RO1,RO2,RO3' REPRESENT DENSITIES
C   OF THE THREE MEDIA. 'MAXFR' IS THE MAXIMUM FREQUENCY PLOTTED.
C
C   READ(5,8000) EPS,NSIG,MAXFN
C   READ(5,8001) C1,C2,C3,THICK,MAXFR
C   READ(5,8002) RO1,RO2,RO3
C   MAXFN1=MAXFN
C   TWOPI=2.*3.14159
C   DUMMY4=MAXFR*.001
C   WRITE(6,9000) C1,C2,C3,THICK
C   WRITE(6,9005) RO1,RO2,RO3
C   WRITE(6,9001) DUMMY4
C   WRITE(6,9002) EPS,NSIG,MAXFN
C
C   CALCULATE CUTOFF FREQUENCY FOR MODE M, STORE IN FC(M),
C   AND WRITE RESULTS FOR EACH MODE TO BE PLOTTED.
C
C   M=2
C   FC(1)=0.
29 ANUM=2.*(M-1.)
   DENOM=4.*THICK*SQRT(1./C2**2-1./C1**2)

```

Figure 16. FORTRAN listing of root-finding computer program AXIAL.

```

FC(M)=ANUM/DENOM
FCM=FC(M)
IF (FCM .GT. MAXFR) GO TO 30
WRITE(6,9004) M,FCM
M=M+1
IF(M .GT. 10) GO TO 7000
GO TO 29
7000 WRITE(6,9020)
C
C 'FREQ' IS THE INITIAL FREQUENCY, 'P' IS THE FREQUENCY INCREMENT,
C WRITE TOTAL NUMBER OF MODES TO BE PLOTTED
C
30 FREQ=100.
P=(MAXFR-FREQ)/200.
X=M-1.
NMODE=IFIX(X)
WRITE(6,9009) NMODE
C
C MAIN LOOP ITERATED FOR 200 FREQUENCIES.
C
DO 5 I=1,200
J=0
FRQ(I)=FREQ
GAM1(I)=TWOPI*FREQ/C1
GAM2(I)=TWOPI*FREQ/C2
GAM3(I)=TWOPI*FREQ/C3
GAM1I=GAM1(I)
GAM2I=GAM2(I)
GAM3I=GAM3(I)
C
C BELOW CUTOFF FREQUENCY FC(M) THE MTH MODE IS INITIALIZED TO THE
C WAVENUMBER IN MEDIUM 1...GAM1I=TWOPI*FREQ/C1.
C
DO 50 N=1,NMODE
TRAP(N,I)=GAM1I
CONTINUE
50
C
C SELECT ENDPOINTS OF INTERVAL TO BE SENT TO ZBRENT.
C
40 J=J+1
A=GAM1I+.0001
B=GAM2I-.0001
IF(J .GT. 1) B=SQRT(GAM2I**2-(TWOPI*(J-1.)*2./(4.*THICK))**2)-.01
IF (FREQ .GT. FC(J+1)) A=SQRT(GAM2I**2-(TWOPI*(J*2. )/(4.*THICK)
C)**2)+.01
FA=F(A)
FB=F(B)
IF(FA*FB .LT. 0.) GO TO 10
C
C IF F(A) AND F(B) HAVE THE SAME SIGN THEN NO ROOT EXISTS IN THAT
C INTERVAL. GO ON TO NEXT MODE OR FREQUENCY.
C
GO TO 41
10 MAXFN=MAXFN1
C
C 'ZBRENT' IS AN IMSL SUBROUTINE WHICH LOCATES THE ROOT OF AN
C EXTERNAL FUNCTION 'F(X)' BETWEEN ENDPOINTS 'A' AND 'B'.
C THE ROOT IS RETURNED AS THE VALUE 'B' SUCH THAT 'F(B)=0'.
C

```

Figure 16. (continued)

```

CALL ZBRENT(F, EPS, NSIG, A, B, MAXFN, IER)
IF(IER .EQ. 129) GO TO 20
C
C
STORE ROOTS FOR MODE J, FREQUENCY I IN 'TRAP'.
TRAP(J,I)=B
41 IF(FREQ .GT. FC(J+1)) GO TO 40
GO TO 4
20 WRITE(6, 9006) MAXFN, I
4   FREQ=FREQ+P
5   CONTINUE
C
C
BEGIN PLOTTING FREQUENCY VS. AXIAL WAVENUMBER VIA 'CALCOMP'
GRAPHICS SUBROUTINES.....
C
C
PLOT GAM2 FIRST SINCE IT HAS THE LARGEST WINDOW. THEN PLOT
GAM1 AND GAM3. USE SCALE AND TRANSLATION FACTORS STORED IN
GAM2(202) AND GAM2(201).
C
C
CALL PLTTY(4662, 6, 7)
CALL START
C
C
MOVE ORIGIN 4.0 IN. OVER AND 2.0 IN. UP FROM LOWER LEFT CORNER.
CALL PLOT(4.0, 2.0, -3)
CALL SCALE(GAM2, 9.0, 200, 1)
CALL SCALE(FRQ, 6.5, 200, 1)
CALL AXIS(0.0, 0.0, 'WAVENUMBER IN Z-DIRECTION', -25, 9.0, 0.0,
CGAM2(201), GAM2(202))
CALL AXIS(0.0, 0.0, 'FREQUENCY', 9, 6.5, 90., FRQ(201), FRQ(202))
CALL DATE(DA)
CALL SYMBOL(-1.75, -1.75, .125, DA, 0., 8)
CALL LINE(GAM2, FRQ, 200, 1, 0, 3)
C
C
GAM1(201)=GAM2(201)
GAM3(201)=GAM2(201)
GAM1(202)=GAM2(202)
GAM3(202)=GAM2(202)
CALL LINE(GAM1, FRQ, 200, 1, 0, 3)
CALL LINE(GAM3, FRQ, 200, 1, 0, 3)
C
C
DO 55 K=1, NMODE
DO 60 I=1, 200
GAM2(I)=TRAP(K, I)
60 CONTINUE
CALL NEWPEN(2) THIS STATEMENT CURRENTLY FOR COMMENT ONLY
CALL LINE(GAM2, FRQ, 200, 1, 0, 3)
55 CONTINUE
C
C
ESTABLISH ARRAYS AND RECORD DATA ON PLOT.
C(1)=C1
C(2)=C2
C(3)=C3

```

Figure 16. (continued)

```

R(1)=RO1
R(2)=RO2
R(3)=RO3
YD=6.5
DO 202 I=1,3
XD=8.0
FLT=C(I)
CALL SYMBOL(XD,YD,0.125,'C=',0.0,2)
CALL NUMBER(999.0,999.0,0.125,FLT,0.0,1)
FLT=R(I)
XD=XD+1.5
CALL SYMBOL(XD,YD,0.125,'RHO=',0.0,4)
CALL NUMBER(999.0,999.0,0.125,FLT,0.0,1)
YD=YD-0.25
202 CONTINUE
XD=8.0
YD=YD-0.25
CALL SYMBOL(XD,YD,0.125,'THICKNESS(M.)=',0.0,15)
CALL NUMBER(999.0,999.0,0.125,THICK,0.0,2)
CALL FINISH
CALL ENDOUT

C
C
C
C
C
8000 FORMAT(F5.3,I2,I3)
8001 FORMAT(5E10.3)
8002 FORMAT(3E10.3)
9000 FORMAT(' C1(M/SEC)=',E11.4,' C2(M/SEC)=',E11.4,' C3(M/SEC)=',
CE11.4,' THICK(M)=',E10.3)
9001 FORMAT(' FREQUENCY RANGE IN KHZ: 0-',E10.3)
9002 FORMAT(' CONVERGENCE CRITERIA FOR ZBRENT: EPS=',F5.3,' NSIG=',I
C2,' MAXFN=',I3)
9004 FORMAT(' MODE M=',I3,' CUTOFF FREQ=',E11.4)
9005 FORMAT(' RO1=',E11.4,' RO2=',E11.4,' RO3=',E11.4)
9006 FORMAT(' ZBRENT FAILED TO CONVERGE IN MAXFN ITERATIONS. MAXFN=',I3
C,' I=',I5)
9009 FORMAT(' TOTAL NUMBER OF MODES M=',I3)
9020 FORMAT(' ERROR.....EXCEEDED DIMENSION FOR TOTAL NUMBER OF MODES.')
STOP
END

C
C
C
C
C
EXTERNAL FUNCTION 'F(X)' IS USED BY ZBRENT TO FIND A ROOT
'B' SUCH THAT 'F(B)=0'.

FUNCTION F(X)
REAL*8 X,F
COMMON/AREA1/GAM1I,GAM2I,GAM3I,RO1,RO2,RO3,I,THICK
DU1=X**2-GAM1I**2
DU2=GAM2I**2-X**2
DU3=X**2-GAM3I**2
IF(DU1.LT.0.) WRITE(6,4000) X,I,GAM1I
IF(DU2.LT.0.) WRITE(6,4001) X,I,GAM2I
IF(DU3.LT.0.) WRITE(6,4002) X,I,GAM3I
ALPH1=SQRT(DU1)

```

Figure 16. (continued)

```

ALPH2=SQRT(DU2)
ALPH3=SQRT(DU3)
G=RO2*RO3*ALPH2*ALPH1+RO2*RO1*ALPH2*ALPH3
H=RO1*RO3*ALPH2**2-RO2**2*ALPH1*ALPH3
F=G*COS(ALPH2*THICK)-SIN(ALPH2*THICK)*H
4000 FORMAT( DU1<0. X=,E11.4, I=,I5, GAM1I=,E11.4)
4001 FORMAT( DU2<0. X=,E11.4, I=,I5, GAM2I=,E11.4)
4002 FORMAT( DU3<0. X=,E11.4, I=,I5, GAM3I=,E11.4)
RETURN
END
//DATA INPUT DD *
0.0 5200
8.0 E03 0.5 E03 8.0 E03 0.1E0 10.1E03
5.0E03 2.0E03 5.0E03
/*

```

Figure 16. (continued)

BIBLIOGRAPHY

- Abramowitz, M., and I.A. Stegun, eds. Handbook of Mathematical Functions. New York: Dover, 1965.
- Berktag, H.O., and C.A. Al-Temimi. "Virtual Arrays for Underwater Reception." Journal of Sound and Vibration, 9 (1969), 295-307.
- Beyer, R.T. Nonlinear Acoustics. Written for Naval Ship Systems Command, Department of the Navy, 1974.
- _____. "Parameter of Nonlinearity in Fluids," Journal of the Acoustical Society of America, 32 (1960), 719-721.
- Blackstock, D.T. "Connection Between the Fay and Fubini Solutions for Plane Sound Waves of Finite-Amplitude." Journal of the Acoustical Society of America, 39 (1966), 1019-1026.
- Budden, K.G. The Wave-Guide Mode Theory of Wave Propagation. New Jersey: Prentice-Hall, 1961.
- Carrier, Krook, and Pearson. Functions of a Complex Variable. New York: McGraw-Hill, 1966.
- Fenlon, F. H. "On the Performance of a Dual Frequency Parametric Source Via Matched Asymptotic Solutions of Burgers' Equation." Journal of the Acoustical Society of America, 55 (1974), 35-46.
- Fenlon, F.H. and D.M. Yeager. "Formation of Parametric Acoustic Arrays in Layered Media." Journal of the Acoustical Society of America, 65, Supplement 1 (1979).
- _____. Class Notes -- Nonlinear Acoustics. The Pennsylvania State University, 1978.
- Ghizoni, C.C., J.M. Ballantyne, and C.L. Tang. "Theory of Optical-Waveguide Distributed Feedback Lasers: A Green's Function Approach." IEEE Journal of Quantum Electronics, 13 (1977). 843-848.
- _____. "Wave-Coupling in Periodic Optical Waveguides." PhD dissertation, Cornell University, 1976.

- Jacobi, W.J. "Propagation of Sound Waves Along Liquid Cylinders." Journal of the Acoustical Society of America, 21 (1949), 120-127.
- Kapany, N.S., and J.J. Burke. Optical Waveguides. New York: Academic Press, 1974.
- King, B.J. "Numerical Investigation of an Acoustic Slow Waveguide." Journal of the Acoustical Society of America, 62 (1977), 1389-1396.
- Knoble, H.D. "Solution of Simultaneous Linear Equations Involving Matrices Whose Elements are Symbolic Multivariate (Complex) Polynomials." Program User's Guide, The Pennsylvania State University Computation Center, 1971.
- Lanczos, C. Linear Differential Operators. London: D. Van Nostrand Co., Ltd., 1961.
- Marcuse, D. Theory of Dielectric Optical Waveguides. New York: Academic Press, 1974.
- Morse, P.M., and K.U. Ingard. Theoretical Acoustics. New York: McGraw-Hill, 1968.
- Nayfeh, A.H. Perturbation Methods. New York: Wiley-Interscience, 1973.
- _____, and M. Tsai. "Nonlinear Acoustic Propagation in Two-Dimensional Ducts." Journal of the Acoustical Society of America, 55 (1974), 1166-1172.
- Ostrovskii, L.A., and I.A. Papilova. "Nonlinear Mode Interaction and Parametric Amplification in Acoustic Waveguides." Soviet Physics-Acoustics, 19 (1973), 45-50.
- Redwood, M. Mechanical Waveguides. New York: Pergamon Press, 1960.
- Rogers, P.H., and W.J. Trott. "Acoustic Slow Waveguide Antenna." Journal of the Acoustical Society of America, 56 (1974), 1111-1117.
- Rudenko, O.V., and S.I. Soluyan. Theoretical Foundations of Nonlinear Acoustics, translated by R.T. Beyer. New York: Plenum, 1977.
- Ryder, J.D., P.H. Rogers, and J. Jarzynski. "Radiation of Difference-Frequency Sound Generated by Nonlinear Interaction in a Silicone Rubber Cylinder." Journal of the Acoustical Society of America, 59 (1976), 1077-1086.

Skudrzyk, E. The Foundations of Acoustics. New York: Springer-Verlag, 1971.

Tien, P.K. "Light Waves in Thin Films and Integrated Optics." Applied Optics, 10 (1971), 2395-2413.

Tolstoy, I. , and C.S. Clay. Ocean Acoustics. New York: McGraw-Hill, 1966.

_____. "Resonant Frequencies and High Modes in Layered Waveguides." Journal of the Acoustical Society of America, 27 (1956), 1182-1192,

_____. "Dispersion and Simple Harmonic Point Sources in Wave Ducts." Journal of the Acoustical Society of America, 27 (1955), 897-907.

Vaidya, P.G., and K.S. Wang. "Nonlinear Propagation of Complex Sound Fields in Rectangular Ducts, Part I: The Self-Excitation Phenomenon." Journal of Sound and Vibration, 50 (1977) 29-42.

walter, C. . Traveling Wave Antennas. New York: McGraw-Hill, 1965.

Westervelt, P.J. "Parametric Acoustic Array." Journal of the Acoustical Society of America, 35 (1963), 535-537.

DISTRIBUTION

Commander (NSEA 09G32)
Naval Sea Systems Command
Department of the Navy
Washington, DC 20362

Copies 1 and 2

Commander (NSEA 0342)
Naval Sea Systems Command
Department of the Navy
Washington, DC 20362

Copies 3 and 4

Defense Technical Information Center
5010 Duke Street
Cameron Station
Alexandria, VA 22314

Copies 5 through 16